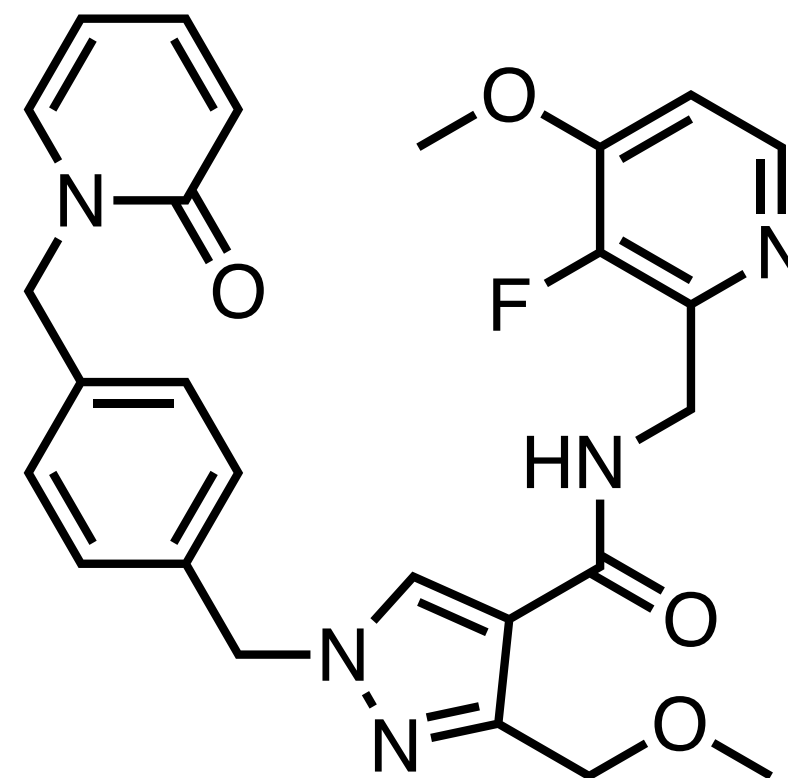


# Small Molecules of the Month

October 2022

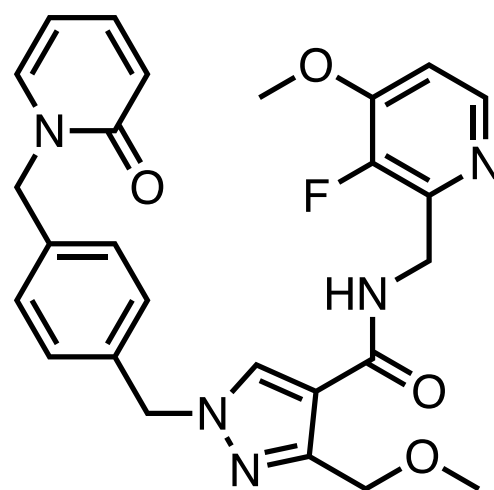
drug  
hunter



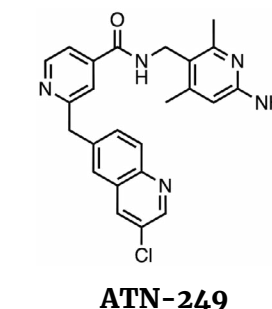
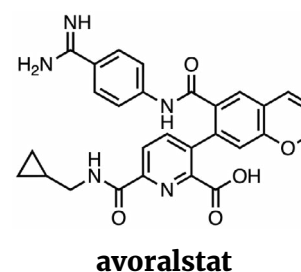
01	sebetralstat	plasma kallikrein	KalVista Pharmaceuticals
02	GDC-2394	NLRP3	Genentech
03	compound 5g	CDK2	Incyte Research Institute
04	AZD1656	glucokinase	AstraZeneca
05	JNJ-64264681	BTK	Janssen R&D
06	BI-0474	KRAS <sup>G12C</sup>	Boehringer Ingelheim
07	compound 57	EGFR <sup>L858R</sup>	F. Hoffmann-La Roche
08	AN15368	CPSF3	Anacor Pharma
09	UCB7362	plasmepsin X	UCB Biopharma
10	BAY-069	BCAT1/2	Bayer Pharma AG

# sebetralstat

## plasma kallikrein



**Context.** [Sebetralstat](#) (KalVista Pharmaceuticals) is an oral, on-demand plasma kallikrein (PKa) inhibitor intended for hereditary angioedema (HAE). As an on-demand medication, it can be administered to treat acute attacks rather than chronically to prevent attacks. Its structure [was first disclosed](#) at the ACS Spring Meeting earlier this year. [HAE](#) is a rare autosomal dominant disease caused by a deficiency in functional [C1 inhibitor](#), a protease inhibitor protein involved in regulation of the complement, contact, and coagulation pathways. Insufficient C1 inhibitor protein results in the inability to suppress PKa activity, causing elevated levels of the vasodilator bradykinin that then leads to painful swelling. This swelling can be life-threatening if localized in the upper airway. Inhibitors of PKa have been [explored](#), with the first approval of the small, 60 amino-acid, 7062 Da protein, [ecallantide](#), granted in 2009. Small molecule inhibitors, including [avoralstat](#), [berotralstat](#), and [ATN-249](#), have reached clinical trials, with berotralstat gaining [FDA approval](#) for prophylactic treatment in late 2020.



**Target/Mechanism of Action.** [Plasma kallikrein](#) is a trypsin-like serine protease that elevates bradykinin levels by cleaving Lys-Arg and Arg-Ser bonds in kininogen to release the vasoactive bradykinin peptide. Inhibition of PKa prevents the elevation of bradykinin. Current approved PKa inhibitors are the biologics [lanadelumab](#) and [ecallantide](#) to treat acute angioedema attacks caused by HAE, and the oral drug [berotralstat](#) as a prophylactic therapy for angioedema attacks.

**Starting Point.** Because PKa substrate selectivity for kininogen depends on interactions with negatively charged residue Asp189 in an S1 subsite, many PKa inhibitors contain basic groups that form a strong salt bridge with this residue. The strongly basic [benzamidine PKa inhibitors](#), “compound 1” and ASP-440 (calculated  $pK_a$  11.6) from ActiveSite Pharmaceuticals, were used as starting points for investigation. However, it can be challenging to identify orally bioavailable basic molecules. Indeed, while both “compound 1” and ASP-440 were potent PKa inhibitors, 5.5 nM and 62 nM, respectively, they lacked oral bioavailability, necessitating the use of a [prodrug approach](#) for ASP-440.

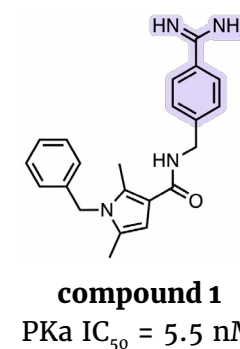
oral, on-demand plasma kallikrein inhibitor  
Ph. III candidate for on-demand treatment  
of HAE attacks

opt. from a known starting point

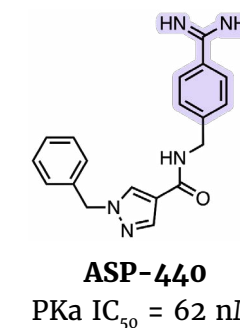
*J. Med. Chem.*

KalVista Pharmaceuticals Ltd., Salisbury, U.K.

paper DOI: <https://doi.org/10.1021/acs.jmedchem.2c00921>



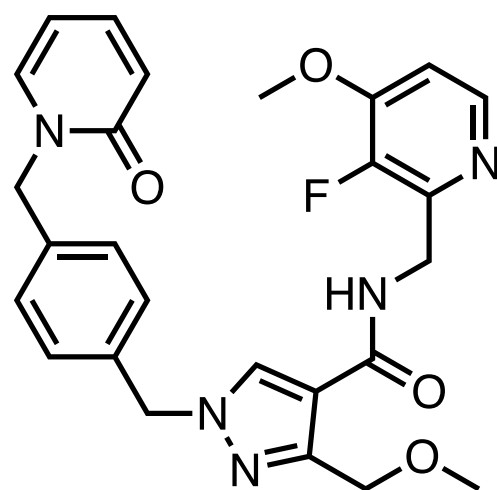
**compound 1**  
PKa  $IC_{50}$  = 5.5 nM



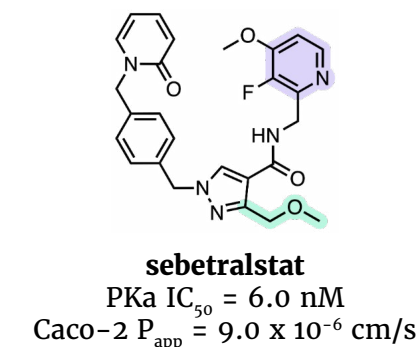
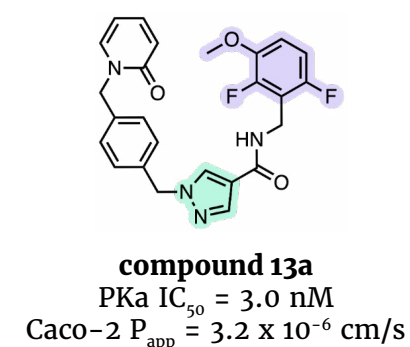
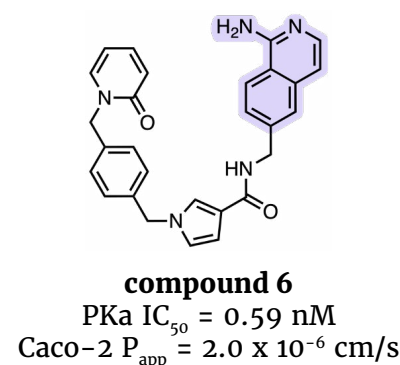
**ASP-440**  
PKa  $IC_{50}$  = 62 nM

# sebetralstat

## plasma kallikrein



**Lead Optimization.** The basic benzamidine group was replaced with an aminoisoquinoline to reduce basicity (calculated  $pK_a$  7.5). Addition of a benzylpyridone seen in “compound 6” led to molecules with picomolar potency (0.59 nM). An amide library was prepared based on “compound 6” as a scaffold with 140 primary amines sourced from the [ZINC database](#) selected based on size ( $MW < 250$ ), properties, and shape. The library was screened using a fluorogenic PKa inhibition assay, leading to the discovery of “compound 13a,” a neutral molecule with comparable inhibitory activity but poor solubility. Addition of a methoxymethylene group on the pyrazole core increased permeability ( $Caco-2 P_{app} = 9 \times 10^{-6}$  cm/s). Replacing the phenyl group with a pyridine ( $pK_a$  3.6) group in sebetralstat improved solubility in simulated gastric fluid (FaSSGF  $>1$  mg/ml). Protonation of pyridine at gastric pH is believed to contribute to its rapid dissolution and absorption in vivo.



**Binding Mode.** The co-crystal structure of sebetralstat bound to PKa (PDB: [8A3Q](#)) is highlighted by an induced U-shaped conformation around its pyrazole core to form a series of  $\pi-\pi$  stacking interactions with Trp215, which adopts an unusual flipped pose for serine proteases. Due to the low basicity of the pyridine, there is no salt bridge between Asp189 and sebetralstat, unlike for past inhibitors. Computational [SiteMap](#) and [WaterMap](#) studies from [Schrödinger](#) were used to explain the binding potency in the absence of a basic group. WaterMap revealed a “hot” or unfavorable, high-energy water above Tyr228 that was not detected in the co-crystal structure. Displacement of the hot water by the methoxy P1 group on sebetralstat is speculated to contribute to the binding affinity.

**Preclinical Pharmacology.** Sebetralstat acted as a reversible PKa inhibitor (whole plasma  $IC_{50} = 54$  nM,  $K_i = 3.0$  nM) with fast kinetics ( $k_{on} > 10 \times 10^6 M^{-1} s^{-1}$ ) and prevented activation of the kallikrein-kinin system in a dextran sulfate (DXS)-activated whole human plasma assay. This assay was developed to mimic kallikrein-kinin system activation during an HAE attack. Furthermore, sebetralstat demonstrated a good PK profile ( $CL_p = 8.7$  mL/min/kg,  $t_{1/2} = 1.0$  hr, and  $F = 34\%$ ) in canines. Sebetralstat showed no significant hERG activity by patch-clamp ( $IC_{50} > 33 \mu M$ ), no genotoxicity in the Ames test, or inhibitory activity against a panel of CYP enzymes. There was a  $>1667$ -fold difference between plasma kallikrein and an extended panel of related human serine proteases, including tissue kallikrein ( $>6667$ -fold). Sebetralstat was nominated for clinical trials over other leads in the series because of its low clearance, high solubility, and high potency in the human PKa plasma activation assay.

**Clinical Development.** Sebetralstat has completed Ph. I ([NCT04349800](#)) and Ph. II ([NCT04208412](#)) clinical trials for on-demand treatment of angioedema attacks in adults with HAE type I or II. Results from the [Ph. II study](#) demonstrated statistically and clinically significant efficacy for all endpoints ( $p < 0.0001$ ) after a single dose of sebetralstat (600 mg), reducing the median time to onset of symptom relief to 1.6 h compared to 9 h with placebo. There were no significant adverse effects reported. A Ph. III trial (300 and 600 mg) is currently underway ([NCT05259917](#)), with subtrials on PK in adolescents ([NCT05511922](#)) and on long-term efficacy in support of a [planned NDA filing](#), as well as data on the feasibility of expanding HAE treatment to younger patients (ages 12–17, [NCT05505916](#)).

**Patent.** Sebetralstat and its analogs were disclosed in the patent [WO2016083820A1](#). The US patent [US10364238B2](#) was granted to Kalvista in July 2019 and is valid until November 2035.

oral, on-demand plasma kallikrein inhibitor  
Ph. III candidate for on-demand treatment  
of HAE attacks

opt. from a known starting point

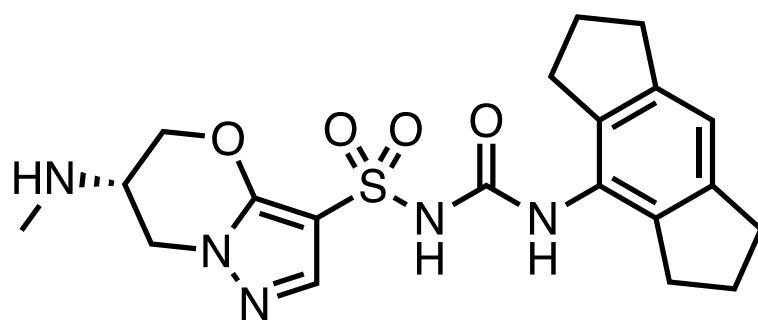
*J. Med. Chem.*

KalVista Pharmaceuticals Ltd., Salisbury, U.K.

paper DOI: <https://doi.org/10.1021/acs.jmedchem.2c00921>

# GDC-2394

## NLRP3



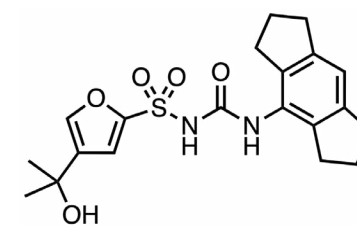
**Context.** [GDC-2394](#) (Genentech) is an oral NLRP3 inflammasome inhibitor. The NLRP3 inflammasome is the [best studied](#) and most characterized [inflammasome](#), with the protein playing a key role in the detection of inflammatory [danger signals](#) which are a hallmark of many inflammatory diseases. Hyperactivation of the NLRP3 has been [implicated](#) in the pathogenesis of several diseases of high unmet need, such as autoimmune, chronic inflammatory, and metabolic diseases, making the protein an [actively pursued](#) drug target. Despite its appeal, development of agents targeting NLRP3 over the years has been challenged by, among other factors, the [scarcity of detailed structural data](#). The first NLRP3 inhibitor to enter the clinic, Pfizer's [CP-456773](#) ([MCC950](#), CRID3), was not realized to be an NLRP3 inhibitor at the time, and was limited by [hepatotoxicity](#) at high doses, triggering research efforts to develop [next generation agents](#). GDC-2394 has reduced lipophilicity and improved potency compared with CP-456773, which is expected to reduce the total effective dose and may lower the risk of drug-induced liver injury.

**Editor Commentary.** Our thanks to [Bryan McKibben](#), one of our [featured reviewers](#), for suggesting this molecule and providing technical feedback.

**Target.** The cytosolic innate immune signaling receptor NLRP3 is a [NOD-like receptor](#) expressed in the cytoplasm of monocytes, neutrophils, dendritic cells, lymphocytes, osteoblasts, and epithelial cells. [Activation of NLRP3](#) triggers assembly of its inflammasome, characterized by caspase-1-mediated activation of IL-1 $\beta$  and IL-8, resulting in induction of inflammatory, pyroptotic cell death. Aberrant NLRP3 activity has been implicated in a [wide range of human diseases](#) including diabetes, atherosclerosis, metabolic syndrome, cardiovascular, and neurodegenerative diseases. In animal studies, both pharmacological inhibition of the receptor and its genetic ablation have been [shown](#) to mitigate NLRP3 inflammasome-mediated inflammation.

**Mechanism of Action.** In line with [other NLRP3 inhibitors](#), GDC-2394 was found to exert its anti-inflammatory effects by inhibiting IL-1 $\beta$  production. The investigators confirmed the drug's mechanism of action through in vivo experiments in an acute mouse peritonitis model, and through in vitro assays in human and mouse whole blood and human macrophages after activation of the NLRP3 inflammasome with lipopolysaccharides, ATP, and/or [cholesterol crystals](#).

**Hit-Finding Strategy.** CP-456773 (MCC950, CRID3), a Pfizer candidate [first disclosed](#) in 1998, was identified following a [phenotypic screen](#), in stimulated monocytes, of compounds that suppressed IL-1 $\beta$  release ( $IC_{50}$  = 29 nM). It was advanced to Ph. II trials in rheumatoid arthritis, but a finding of elevated transaminases in patients taking high doses [halted further development](#). The exact nature of this toxicity remains undisclosed, however, drugs with high lipophilicity ( $LogP \geq 3$ ), taken at high daily doses ( $\geq 100$  mg/day) are known to [increase risk](#) for [drug-induced liver injury](#) (DILI). Given its promise, CP-456773 was used as a starting point, with a goal of reducing lipophilicity and improving potency, such that the total daily dose could be reduced.



**CP-456773**

IL-1 $\beta$   $IC_{50}$  = 0.029  $\mu$ M  
LLE = 7.0

oral NLRP3 inhibitor

predicted human dose of 500 mg QD

LLE opt. and tox. mitig. from prev. clin. cand.

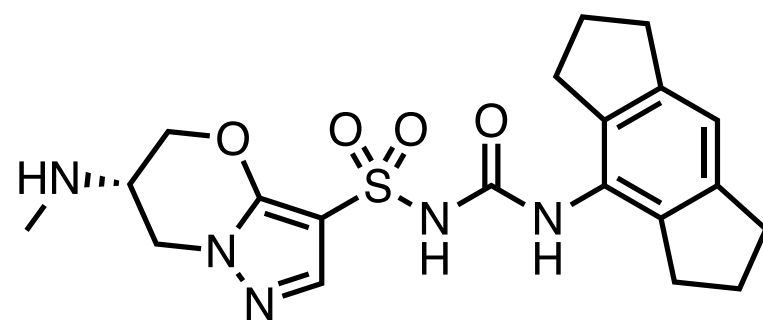
*J. Med. Chem.*

Genentech, South San Francisco, CA

paper DOI: <https://doi.org/10.1021/acs.jmedchem.2c01250>

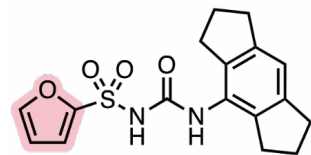
# GDC-2394

## NLRP3



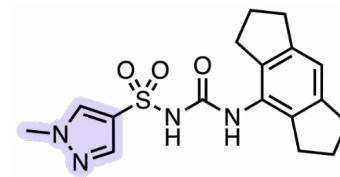
**Lead Optimization.** A [lipophilic ligand efficiency](#) (LLE)-focused approach was used to optimize CP-456773. Furthermore, the furan moiety was identified as a candidate for replacement, as they can be toxicophores and have been [associated](#) with DILI. Using a ligand-based design campaign, a number of aryl and heteroaryl moieties were investigated as a replacement for the furan. Compounds were assessed using an assay that quantified IL-1 $\beta$  release from nigericin-stimulated human immune cells (PBMCs) as a measure of NLRP3 activity. A counter screen looking at TNF $\alpha$  levels was performed to rule out inhibition of the TLR4/NF $\kappa$ B signaling pathway, which is necessary for proper NLRP3 function, as well as a CellTiter-Glo assay to ensure decreases in IL-1 $\beta$  were not due to general toxicity.

LLE-guided substitution of the furan with benzene, pyridine, or pyrazine led a decrease in activity, as did substitution with dimethylimidazole. However, *N*-methyl pyrazole (“compound 13”) provided an interesting lead, exceeding both the potency and LLE of the unsubstituted furan (“compound 2”). Further optimization of the pyrazole led to “compound 17”, which accomplished the goal of finding a suitable furan replacement. Initial in vitro studies showed that “compound 17” had whole blood properties comparable with CP-456733, and showed no safety signals in hERG, BSEP, cytotoxicity, and GSH trapping assays. However, renal toxicity was observed in cyno monkeys after oral dosing at  $\geq 100$  mg/kg/day for 14 days. Subsequent SAR investigations indicated the 6-position of the oxazine ring accommodated a range of substitutions, with the (*S*)-amino methyl moiety (GDC-2394) providing the best overall properties.



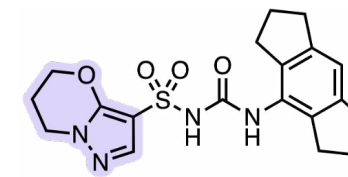
**compound 2**

IL-1 $\beta$  IC<sub>50</sub> = 0.44  $\mu$ M  
LLE = 5.7



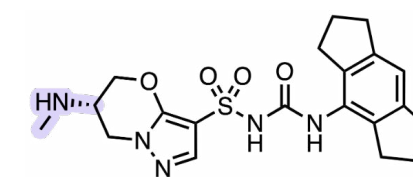
**compound 13**

IL-1 $\beta$  IC<sub>50</sub> = 0.21  $\mu$ M  
LLE = 6.3



**compound 17**

IL-1 $\beta$  IC<sub>50</sub> = 0.063  $\mu$ M  
LLE = 6.7



**GDC-2394**

IL-1 $\beta$  IC<sub>50</sub> = 0.0054  $\mu$ M  
LLE = 8.2

**Binding Mode.** A cryo-EM structure ([PDB:8ETR](#)) revealed an allosteric binding mode for GDC-2394. The ligand-NLRP3 interaction occurs at the intersection of HD1, HD2, NBD, and WHD subdomains of the [NACHT domain](#). The urea and sulfonamide cores, positioned between the HD2 and NBD narrow channel, are essential to inhibitor activity, making several interactions with nearby residues. The increase in potency observed upon addition of the oxazine ring can be rationalized as due to a hydrogen bond between the oxygen atom and Arg578 residue.

**Preclinical Pharmacology.** In an acute mouse peritonitis model, 1 and 10 mg/kg of the compound resulted in the reduction of IL-1 $\beta$  levels by 66.3% and 81.3%, respectively ( $P < 0.001$ ). Furthermore, in a functional rat model of gouty arthritis, knee swelling in the animals was significantly reduced with GDC-2394 treatment after 48 h vs. vehicle treatment ( $P < 0.001$ ), with an inhibitory effect observed through day 6 of the study. A human whole blood assay was used to predict a human QD dose of 500 mg QD (covering the IC<sub>50</sub>). PK predictions also suggested an oral bioavailability of 61%, a half-life of 2.3 h, and clearance of 1.5 mL/min/kg.

**Clinical Development.** Preclinical compound.

**Patent.** GDC-2394, and its analogs with NLRP3-modulating activity, were described in the patent [WO2018136890A1](#). The US patent [US11040985B2](#) was granted to Genentech in June 2021 and is valid until February 2038.

oral NLRP3 inhibitor

predicted human dose of 500 mg QD

LLE opt. and tox. mitig. from prev. clin. cand.

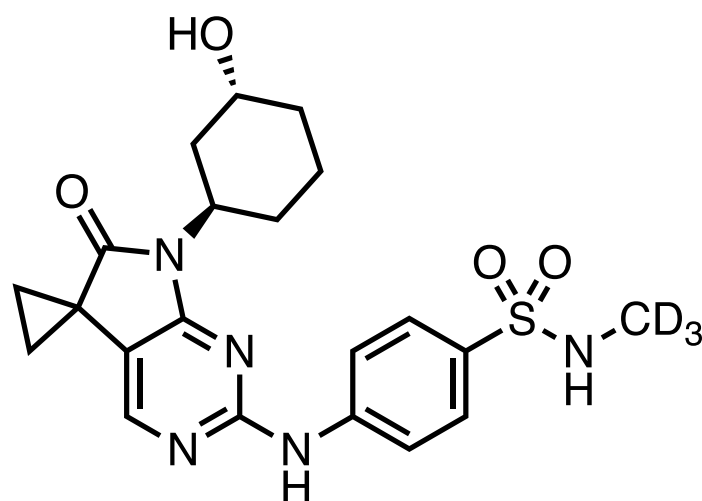
*J. Med. Chem.*

Genentech, South San Francisco, CA

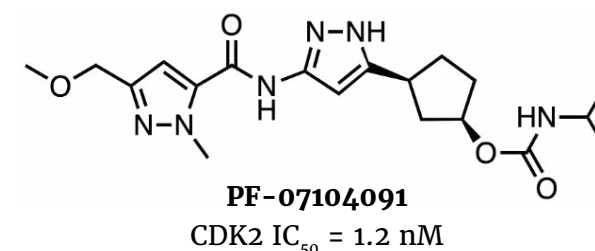
paper DOI: <https://doi.org/10.1021/acs.jmedchem.2c01250>

# compound 5g

## CDK2



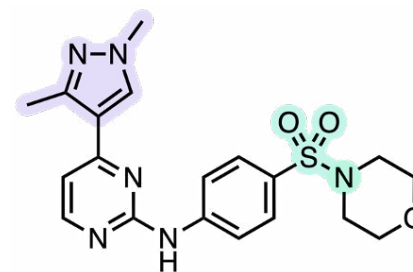
**Context.** “Compound 5g” (Incyte) is a selective CDK2 kinase inhibitor. Although CDK2 is a [highly pursued cancer drug target](#), inhibitors targeting the key cell cycle regulator have not enjoyed similar success as [CDK4/6 inhibitors](#), in part due to the major challenge of mitigating off-target CDK1/9 activity through the use of highly selective agents. Given recent [data](#) suggesting that resistance to approved CDK4/6 inhibitors may involve a CDK2-mediated compensatory pathway, CDK2 inhibitors may additionally address an unmet need for patients who progress following CDK4/6 therapy. Scaffold hopping on an HTS hit led to “compound 5g” containing the 5,7-dihydro-6H-pyrrolo[2,3-d]pyrimidin-6-one core structure. The compound demonstrated high selectivity (>200x) for CDKs 1/4/6/7/9 and showed submicromolar in vitro activity. Currently, the most advanced CDK2 inhibitor appears to be Pfizer’s PF-07104091 which is being [evaluated](#) in both a single agent and combination therapies in Ph. I/II studies.



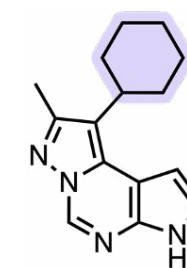
PF-07104091  
CDK2 IC<sub>50</sub> = 1.2 nM

**Target.** As a key regulator of cell cycle progression, CDK2, like other CDKs, is a [well-studied](#) oncotarget, although [off-target effects](#) of early CDK2 inhibitors dampened interest in this target. However, newly found roles for the protein, such as its [reported](#) involvement in compensatory pathways that mediate resistance to currently approved CDK4/6 inhibitors, have [reignited interest](#) in the cancer target. Incyte scientists aimed to develop a compound with nanomolar activity against CDK2 and concomitant >100x selectivity against CDK1/4/6/7/9.

**Hit-Finding Strategy.** A high-throughput screen of Incyte’s in-house library identified “compound 1a” (IC<sub>50</sub> = 431 nM) and “compound 1b” (IC<sub>50</sub> = 2.8 μM) as CDK2 hits. The library was screened at 1 mM ATP in a CDK2/cyclin E1 homogeneous time-resolved fluorescence (HTRF) binding assay, using eIF4E-binding protein peptide as substrate. In addition to “compound 1a” and “compound 1b”, the screen identified a number of related pyrazole congeners with varying substituents at the 1- position. It was reasoned that an appropriately placed lipophilic moiety off the 4-position of the pyrimidine and the aryl sulfonamide were responsible for the potency seen in “compound 1a”. Although “compound 1b” was less potent, they further reasoned that the rigid, tricyclic ring system placed the cyclohexyl substituent into a similar area of space as the pyrazole, and could be the reason for the observed activity.



compound 1a  
CDK2/E1 IC<sub>50</sub> = 431 nM



compound 1b  
CDK2/E1 IC<sub>50</sub> = 2.8 μM

oral CDK2 Inhibitor

oral/IV PK observed in rats

in-house HTS and scaffold hopping

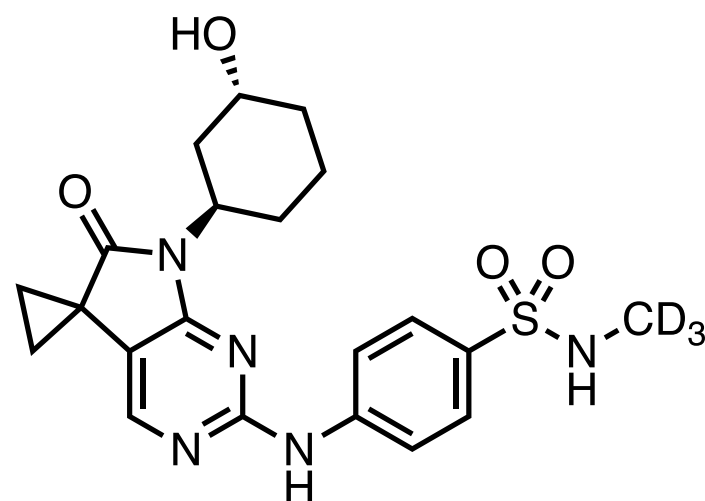
ACS Med. Chem. Lett.

Incyte Research Institute, Wilmington, DE

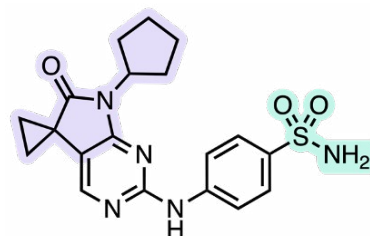
paper DOI: <https://doi.org/10.1021/acsmchemlett.2c00408>

# compound 5g

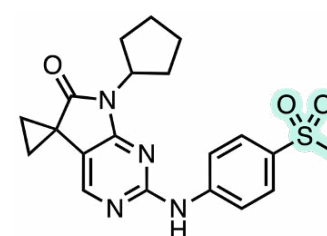
## CDK2



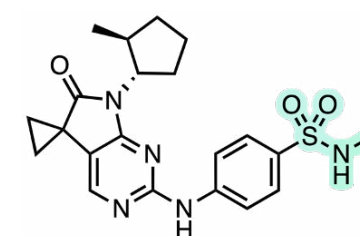
**Lead Optimization.** Initial attempts to maximize selectivity against other CDKs began with merging the two scaffolds from “compound 1a” and “compound 1b” to form a sulfonamide with a bicyclic core. Installation of a bicyclic  $\gamma$ -lactam in “compound 2c” was hypothesized to play a key role in conformational rigidity to create distinct but minor differences in the CDK family binding pocket, imparting selectivity for CDK2 vs. CDK1 (245-fold). However, in the presence of whole blood (hWB), potency loss (7600 nM) was observed due to [primary sulfonamide’s propensity to bind to erythrocytes](#). Moving to a methyl sulfonate (“compound 3a”) showed promise, but cellular potency was again lacking (data not provided). SAR studies on the sulfonamide revealed sensitivity to any polar groups or substituents larger than a methyl, which necessitated a shift to a deuterated methyl functionality to [deter sulfonamide dealkylation](#) and improve microsomal stability ( $Cl_{hu} = 0.7$  L/h/kg). A final optimization of the lactam substituent provided “compound 5g”, which exhibited excellent potency (CDK2  $IC_{50} = 0.3$  nM) and selectivity against CDK1 (1200-fold) and other CDKs (>200-fold).



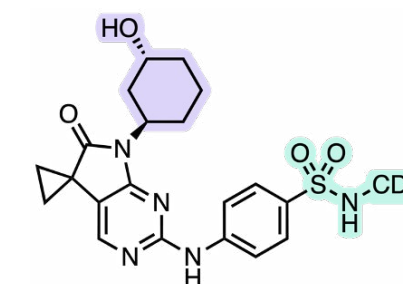
**compound 2c**  
CDK2/E1  $IC_{50} = 4.9$  nM  
CDK1  $IC_{50} = 1200$  nM (245x)  
hWB  $IC_{50} = 7600$  nM



**compound 3a**  
CDK2/E1  $IC_{50} = 102$  nM  
CDK1  $IC_{50} = >5$   $\mu$ M



**compound 4a**  
CDK2/E1  $IC_{50} = 0.33$  nM  
CDK1  $IC_{50} = 294$  nM (890x)  
hWB  $IC_{50} = 230$  nM



**compound 5g**  
CDK2/E1  $IC_{50} = 0.3$  nM  
CDK1  $IC_{50} = 360$  nM (1200x)  
hWB  $IC_{50} = 642$  nM

**Binding Mode.** X-ray crystal structure not disclosed.

**Preclinical Pharmacology.** The compound exhibited submicromolar in vitro potency (642 nM) and demonstrated selectivity of 1200x, 17000x, and 8200x against CDK1, CDK7, and CDK9, respectively. Against CDK4 and CDK6, the compound showed selectivity of 770x and 230x, respectively. In vivo efficacy and safety data have not been reported.

**Clinical Development.** Preclinical compound.

**Patent.** Compound 5g and related CDK2 inhibitors were disclosed in the patent [WO2020205560A1](#). US patent [US20200399273A1](#) was filed by Incyte in March 2020 and is still pending.

oral CDK2 Inhibitor

oral/IV PK observed in rats

in-house HTS and scaffold hopping

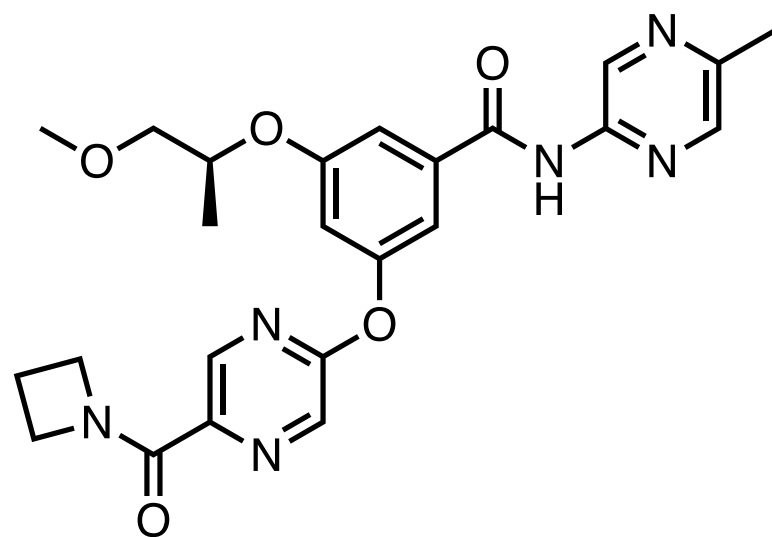
*ACS Med. Chem. Lett.*

Incyte Research Institute, Wilmington, DE

paper DOI: <https://doi.org/10.1021/acsmchemlett.2c00408>

# AZD1656

## glucokinase

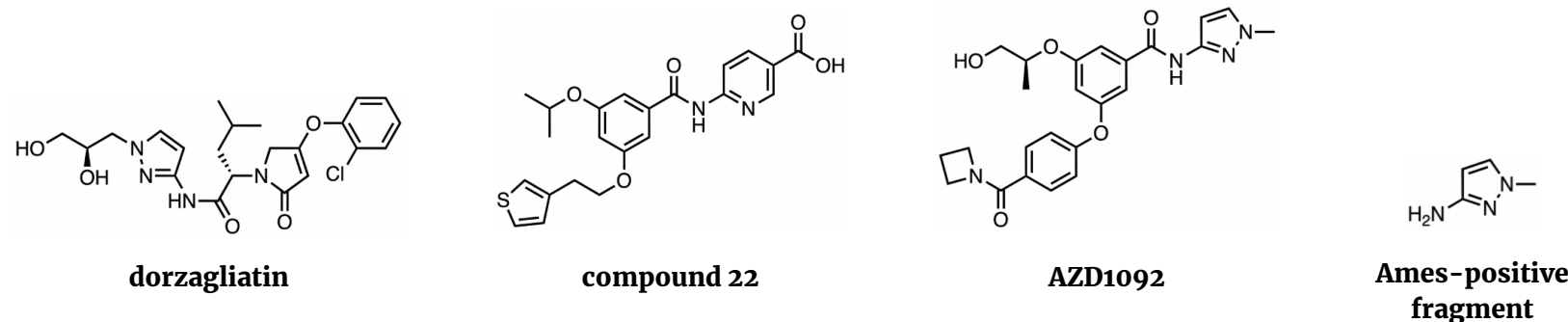


**Context.** [AZD1656](#) (AstraZeneca) is an oral glucokinase (GK) activator (GKA) for hyperglycemia in type 2 diabetes mellitus. Despite GK being [first reported](#) more than 50 years ago and [subsequent extensive research efforts](#), a GKA is yet to be approved. Most GKAs have [failed](#) in clinical development owing to an increased risk of hypoglycemia and gradual loss of efficacy. Consequently, alternative strategies such as the development of [hepatoselective molecules](#) and [partial activation](#) of the enzyme have been tried, with some of these agents still in clinical development. Previously, we [covered](#) dorzagliatin (Hua Medicine), a hepatic and pancreatic dual-acting full GKA that is currently the most advanced in the class. AZD1656, a full GKA, was [first reported](#) 10 years ago and has been evaluated in more than [20 Ph. I/II studies](#). Although the compound is currently not listed among AstraZeneca's cardiovascular, renal, and metabolism pipeline, the [newly reported data](#) by the company on the amenability of GKAs to chronotherapy (scheduled drug administration) may offer an opportunity to revisit the dosing scheme of AZD1656 to ensure better glycemic tolerance/control and increased insulin sensitivity. In addition to improved glucose control, the timing of AZD1656 treatment to feeding times in obese rats led to improvements in hepatic steatosis, inflammation, and fibrosis.

**Target.** [GK](#) is a member of the hexokinase family which phosphorylates glucose to glucose-6-phosphate (G6P) in hepatocytes and pancreatic  $\beta$ -cells. The enzyme's low affinity for glucose ( $K_m = \sim 8$  mM) ensures that it is not saturated at physiological glucose levels ( $\sim 5$  mM), allowing it to act as a glucose "sensor." Loss-of-function GK mutations have been [shown](#) to cause early-onset non-insulin-dependent diabetes mellitus, while gain-of-function mutations have been [linked](#) with hyperglycemia.

**Chronotherapy.** AstraZeneca scientists [found that](#) GK demonstrates a circadian expression pattern in mouse hepatocytes, where its expression was highest during the dark cycle, which is the typical feeding period of rodents. Glucokinase activation during feeding improved glucose control, insulin resistance, hepatic steatosis, inflammation, and fibrosis; abstaining from drug administration during fasted periods avoids the promotion of glucose oxidation and lipid storage. On the other hand, continuous activation eventually manifested in severe liver steatosis, likely due to a contradiction in the normal metabolic state.

**Hit-Finding Strategy.** A glucokinase inhibitor (AZD1092, 30 nM) was previously [disclosed](#) by AstraZeneca following initial optimization of a hit ("compound 22") [discovered](#) by a high throughput screen the company's in-house library. The [assay](#) measured the enzymatic activity of recombinant human pancreatic GK by following the rate of G6P formation. In progressing AZD1092 to clinical trials, a potential hydrolysis fragment was positive in the Ames assay. Although this fragment was never observed in preclinical PK studies, the potential for costly, front-loaded genotoxicity tests and delayed clinical progression made a follow up campaign that would address these issues more palatable.



oral glucokinase activator

Ph. II in renal transplant patients with DM2

AZD1092 opt. to avoid Ames test liability

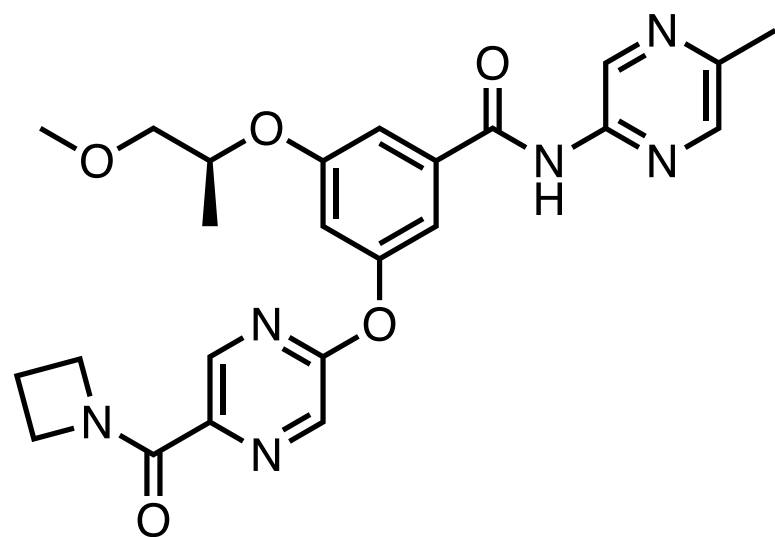
*Sci. Transl. Med.*

AstraZeneca, Gothenburg, SE

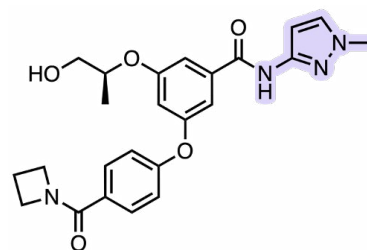
paper DOI: <https://doi.org/10.1126/scitranslmed.abh1316>

# AZD1656

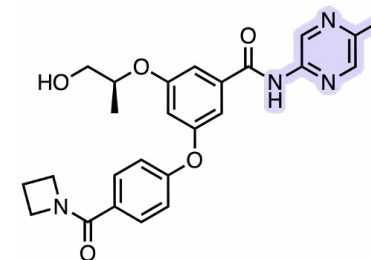
## glucokinase



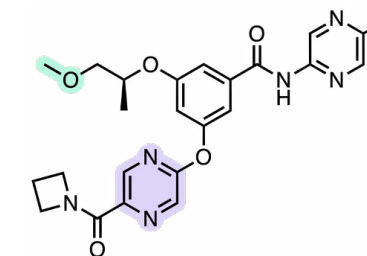
**Lead Optimization.** Replacement of the 1-methyl-3-aminopyrazole in AZD1092 with an aminopyrimidine (“compound 7”) circumvented the positive Ames test but sacrificed some activity, with a twofold drop. An additional concern resulting from this switch is a nearly twofold increase in hERG activity (from 70  $\mu\text{M}$  to 38  $\mu\text{M}$ ), although this was overcome while maintaining potency through methylation of the alcohol and replacing the phenyl ring of the azetidyl benzamide to a 1,4-pyrimidine, bringing hERG activity to greater than 100  $\mu\text{M}$  (AZD1656).



**AZD1092**  
GK  $\text{EC}_{50}$  = 30 nM  
hERG  $\text{IC}_{50}$  = 70  $\mu\text{M}$



**compound 7**  
GK  $\text{EC}_{50}$  = 61 nM  
hERG  $\text{IC}_{50}$  = 38  $\mu\text{M}$



**AZD1656**  
GK  $\text{EC}_{50}$  = 61 nM  
hERG  $\text{IC}_{50}$  = >100  $\mu\text{M}$

**Binding Mode.** The exact binding mode of the AZD1656 has not been disclosed, but glucokinase activators are known to act through an [allosteric site](#), stabilizing the active conformation of the enzyme.

**Preclinical Pharmacology.** Obese male Zucker rats were used in the in vivo studies to evaluate the effects of chronotherapy with differing diurnal exposure profiles on the metabolism of the animals. Tracking the levels of  $^{14}\text{C}$ -glucose and  $^3\text{H}$ -palmitate, administration of AZD1656 led to increased flux of glucose through all major metabolic pathways that utilize glucose, including glycolysis, lactate production, oxidation, and lipogenesis, while fatty acids were typically diverted from oxidation into storage. In dose-response studies, a single oral dose of 21  $\mu\text{mol}/\text{kg}$  was found to show efficacy for  $\geq 8$  h post-administration, reaching non-therapeutic concentrations  $\sim 12$  hours post-dose. This ensured that GK activation was restricted to either the feeding or fasting periods. Timing AZD1656 treatment to feeding periods improved glucose tolerance/control, increased insulin sensitivity, and preserved  $\beta$  cell function. In mice dosed to achieve continuous 24-h therapeutic exposures, liver triglyceride levels were increased by  $\sim 40\%$ , resulting in liver steatosis. When dosing was timed to feeding periods, liver triglyceride levels were reduced by  $\sim 50\%$  vs. vehicle controls and  $\sim 50\%$  vs. animals with continuous exposure. Further, timing treatment to feeding was found to restore postprandial hepatic insulin signaling and support liver lipid exodus.

**Clinical Development.** AstraZeneca has evaluated AZD1656 in [several completed Ph. I and Ph. II studies](#). The Ph. II studies evaluated either AZD1656 monotherapy, in combination with metformin, or combined with insulin. In [NCT01020123](#), 530 patients were randomized to either AZD1656, placebo, or glipizide. The primary endpoint was the placebo-corrected change in HbA1c from baseline to 4 months of treatment. Compared with those who received a placebo, significant HbA1c reductions were seen in the AZD1656 treatment group who received 10–140 mg (mean change:  $-0.80\%$  [95% CI:  $-1.14$ ;  $-0.46$ ]) and 20–200 mg (mean change:  $-0.81\%$  [95% CI:  $-1.14$ ;  $-0.47$ ]); a similar results trend was observed with glipizide. AZD1656 had a favorable safety profile, and fewer patients treated with the drug experienced hypoglycemia vs. glipizide.

**Patent.** AZD1656 and related glucokinase activators were described in the patent [WO2007007041A1](#). The US patent [US7642259B2](#) describes processes for preparing these compounds, while [US8093252B2](#) describes a new polymorphic form of AZD1656 as well as the processes for making it and its use as a glucokinase activator.

oral glucokinase activator

Ph. II in renal transplant patients with DM2

AZD1092 opt. to avoid Ames test liability

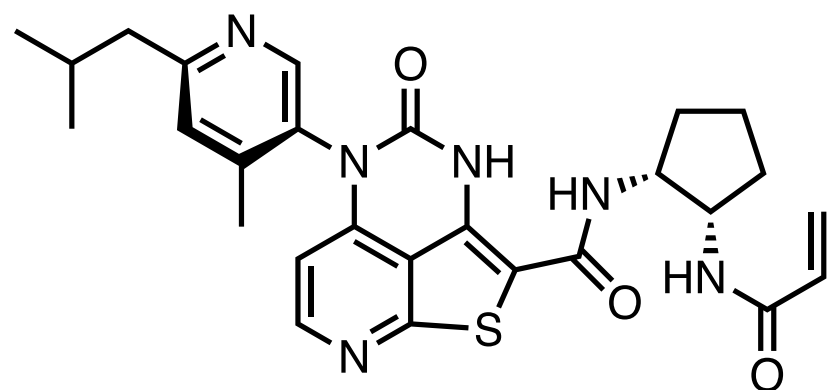
*Sci. Transl. Med.*

AstraZeneca, Gothenburg, SE

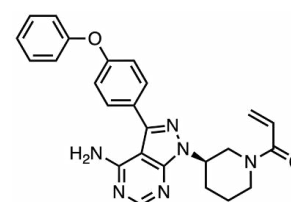
paper DOI: <https://doi.org/10.1126/scitranslmed.abh1316>

# JNJ-64264681

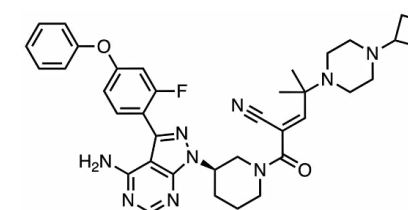
**BTK**



**Context.** [JNJ-64264681](#) (Janssen) is a **covalent** Bruton's tyrosine kinase (BTK) **inhibitor** being developed for hematological malignancies. The first-in-class irreversible BTKi (**ibrutinib**) was approved in 2013, while **many others** have been approved or are in clinical development with potentially reduced **off-target effects**. We **recently covered** another covalent BTKi, **rilzabrutinib**, (PRN1008; Sanofi), currently in Ph. III for immune thrombocytopenia. JNJ-64264681 demonstrates nanomolar oral efficacy in both lymphoma and autoimmune models and improved kinase selectivity. It is currently in **early clinical development** as both a single agent and combination therapy with an aim to reduce adverse effects and patient relapse rates and improve efficacy compared to other BTKi's on the market.



**ibrutinib**



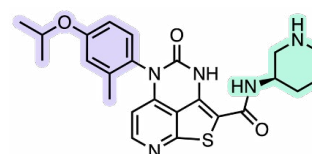
**rilzabrutinib**

**Editor Commentary.** This is an interesting example of an oral clinical candidate with two amides with free N-H donors and an axis of chirality.

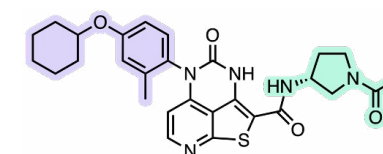
**Target.** A member of the Tec family, **BTK** is a non-receptor cytoplasmic tyrosine kinase and is predominantly expressed in hematopoietic cells, excluding T or NK cells. BTK plays a **key role in B cell development** via B-cell receptor (BCR) activation, a pathway involved with **lymphoma pathogenesis**. Stimulation of BCR in mature B cells **induces BTK phosphorylation**, while **BTK knockout mice** demonstrated aberrant BCR signaling following activation, inducing activation markers, limiting cell division, and increasing susceptibility to apoptosis.

**Mechanism of Action.** As a covalent BTK inhibitor, JNJ-64264681 binds the active site to block B-cell proliferation and pro-survival signals.

**Hit-Finding Strategy and Hit-to-Lead.** Parent "**compound 9**" was disclosed in 2021 as an ATP-competitive inhibitor of BTK with micromolar affinity in a Lanthascreen binding assay screen of Janssen's compound collection. The addition of an acrylamide moiety to the piperidine nitrogen increased potency by 30-fold, and para-phenoxy and ortho-methyl groups on the phenyl ring that fill the back-pocket region further improved the properties overall, resulting in the \*S atropisomer ("**compound 1**") as the most potent compound with the highest barrier of interconversion among the analogs/isomers investigated. **As we recently covered**, drug candidates that exist as atropisomers should have a high barrier to rotation and a corresponding long half-life for interconversion to ensure optimal developability. The acrylamide linker was modified to an amino-pyrrolidine to optimize the covalent modification of Cys481, resulting in "compound 1" that was still limited by low oral bioavailability and aqueous stability when dosed as a crystalline suspension.



**compound 9**  
BTK IC<sub>50</sub> = 3.5 μM



**compound 1**  
pH 2/7 solubility = <4/<4 μM  
rat WB IC<sub>50</sub> = 130 nM  
hWB IC<sub>50</sub> = 84 nM

oral BTK inhibitor

Ph. I candidate in NHL/CLL patients

from Janssen cmp. collection screen and opt.

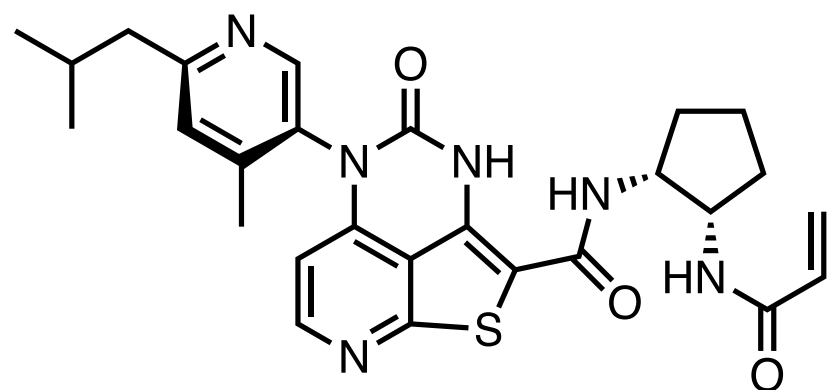
*J. Med. Chem.*

Janssen, San Diego, CA

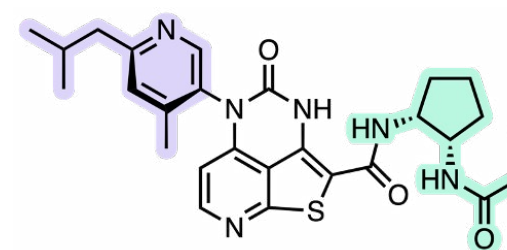
paper DOI: <https://doi.org/10.1021/acs.jmedchem.2c01026>

# JNJ-64264681

**BTK**



**Lead Optimization.** Optimization efforts focused on improving aqueous stability by reducing LogP/lipophilicity and increasing Fsp<sup>3</sup>. The back-pocket biaryl side chain was replaced with a pyridine with aliphatic substituents, retaining the *ortho*-methyl group to preserve the higher potency of the single \*S atropisomer. The acrylamide linker was optimized from an amino-piperidine to a *cis*-diaminocyclopentane resulting in JNJ-64264681 with improved microsomal stability (Human liver microsome T<sub>1/2</sub> of 38 vs. 23 mins), lipophilicity (Log D<sub>7.4</sub> of 3.63 vs. 2.71), Fsp<sup>3</sup> (32% vs. 17%), and aqueous solubility (pH 2/7 of 320/7 vs. <4/<4 μM), as well as improved or maintained in vivo efficacy in the rat and human whole blood assays (130 vs. 41 nM and 84 vs. 89 nM, respectively).



**JNJ-64264681**

pH 2/7 solubility = 320/7 μM

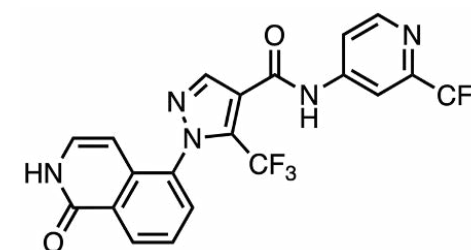
rat WB IC<sub>50</sub> = 41 nM

hWB IC<sub>50</sub> = 89 nM

**Binding Mode.** The X-ray structure of BTK bound with JNJ-64264681 (PDB:8E2M) clearly shows the expected covalent interaction of the acrylamide moiety with the Cys481 residue. Other features of the binding mode include H-bonding interactions between the thienopyridine nitrogen to Met477 and the oxygen of the cyclic urea to Lys430.

**Preclinical Pharmacology.** The antiproliferative activity of JNJ-64264681 was confirmed in vitro using a DLBCL cell line (IC<sub>50</sub> = 18–34 nM) and in vivo using diffuse large B-cell lymphoma (DLBCL) xenograft mice (QD, TGI = 24%, 35%, 51% at 10, 30 and 100 mg/kg; BID, TGI=26%, 51%, and 78% at 5, 15, and 50 mg/kg).

**Clinical Development.** JNJ-64264681 is currently being evaluated in two Ph. I (NCT04210219, NCT04657224) dose escalation and expansion studies. The first is expected to enroll 108 patients with non-Hodgkins lymphoma (NHL) and chronic lymphocytic leukemia (CLL). The second is in combination with JNJ-67856633 (safimaltib), a MALT1 protease inhibitor also being developed by Janssen, and has enrolled 75 patients with NHL and CLL.



**JNJ-67856633**

**Patent.** JNJ-64264681 and related polycyclic BTK inhibitors were disclosed in the patent WO2017100662A1. The US patent US10717745B2 was granted to Janssen Pharmaceutica in July 2020 and is valid until December 2036.

oral BTK inhibitor

Ph. I candidate in NHL/CLL patients

from Janssen cmp. collection screen and opt.

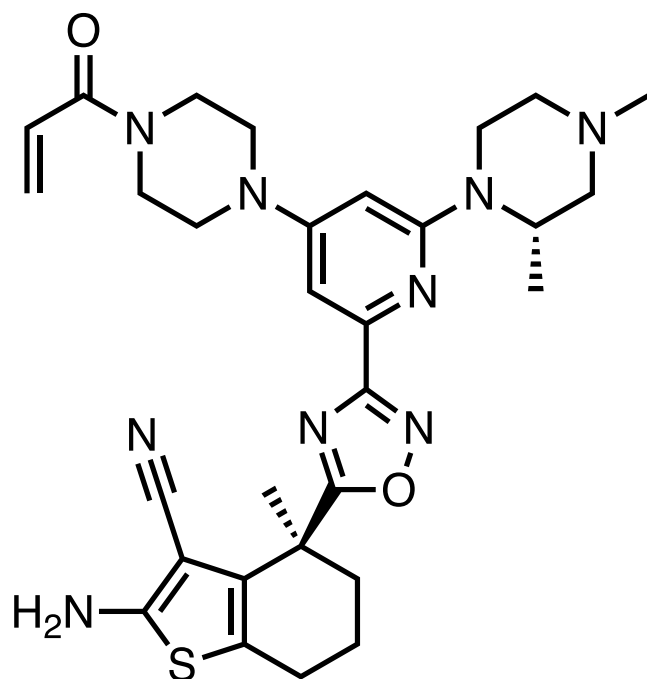
J. Med. Chem.

Janssen, San Diego, CA

paper DOI: <https://doi.org/10.1021/acs.jmedchem.2c01026>

# BI-0474

## KRAS<sup>G12C</sup>

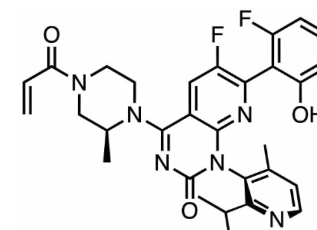


IP KRAS<sup>G12C</sup>i related to oral candidate BI 1823911  
TGI in NCI-H358 cancer xenograft mouse model  
from 13k compd. HSQC-based screen and SBDD  
*J. Med. Chem.*

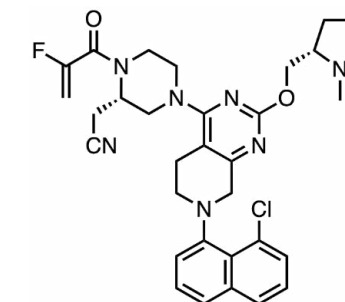
Boehringer Ingelheim, Vienna, AT

paper DOI: <https://doi.org/10.1021/acs.jmedchem.2c01120>

**Context.** BI-0474 (Boehringer Ingelheim) is a covalent KRAS<sup>G12C</sup> inhibitor. KRAS continues to be a **hotly pursued** oncotarget since the **first report** by the Shokat group of the druggability of the KRAS<sup>G12C</sup> mutant. Recently, Amgen's first-in-class **sotorasib** (Lumakras) was approved, while Mirati Therapeutics' adagrasib (MRTX84) **may be approved** in December 2022, based on its PDUFA date. For BI-0474, Boehringer Ingelheim scientists started with a reversible switch II pocket binder and optimized affinity of the reversible molecule via structure-based design before introducing an acrylamide covalent warhead as a last step. While BI-0474 is a non-oral tool molecule, Boehringer Ingelheim mentions an advanced, orally bioavailable compound from the series (BI 1823911) is currently in **early clinical development**. Opportunities for differentiation could be better safety and combinability, such as in lower incidence of hepatotoxicity on combination with immunotherapy, lower total daily dose given the essentially gram-daily doses of the leaders, or greater efficacy due to a different resistance profile.



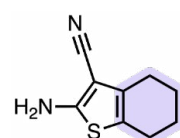
sotorasib



adagrasib

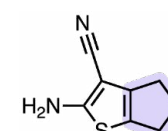
**Target.** KRAS mutations are among the most common cancer-driving mutations. The KRAS<sup>G12C</sup> mutation, which substitutes the native glycine with cysteine, is one of the more **successfully targeted KRAS mutants** due to the ability to target cysteine more readily with covalent molecules. Epidemiological studies have **reported** that the mutation is present at a frequency of 3-14% in NSCLC, colorectal cancer, appendiceal and small bowel cancers, and cancers of unknown primary site.

**Hit-Finding Strategy and Hit-to-Lead.** "Compound 1" was identified following a previous **HSQC-based screen** of ~13,000 fragments that evaluated binders of a nearby subpocket that opens up following covalent modification of the switch I/II pocket in mutant KRAS<sup>G12V,S39C</sup>. The pocket was opened using (1H-benzo[d]imidazol-2-yl)methanethiol (BIT) to bind to an introduced cysteine residue (Cys39), and verified using both NMR and X-ray crystallography. Interestingly, "compound 1" ( $K_D = 116 \mu\text{M}$ ) bound around two-fold better than the five-membered ring analogue "compound 2" ( $K_D = 193 \mu\text{M}$ ), and six-fold better than the aminothiazole "compound 3" ( $K_D = 715 \mu\text{M}$ ). An optimized fragment, "compound 12", was found following X-ray analysis of "compound 1" in complex with GDP•KRAS<sup>G12V,C118S,S39C-BIT</sup>, which revealed the 4-position of the cyclohexyl ring was oriented toward the G12V-position of the protein (**PDB:7U8H**).



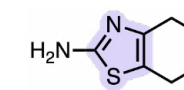
compound 1

KRAS<sup>G12V,S39C</sup>-BIT  $K_D = 116 \mu\text{M}$



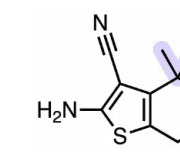
compound 2

KRAS<sup>G12V,S39C</sup>-BIT  $K_D = 193 \mu\text{M}$



compound 3

KRAS<sup>G12V,S39C</sup>-BIT  $K_D = 715 \mu\text{M}$

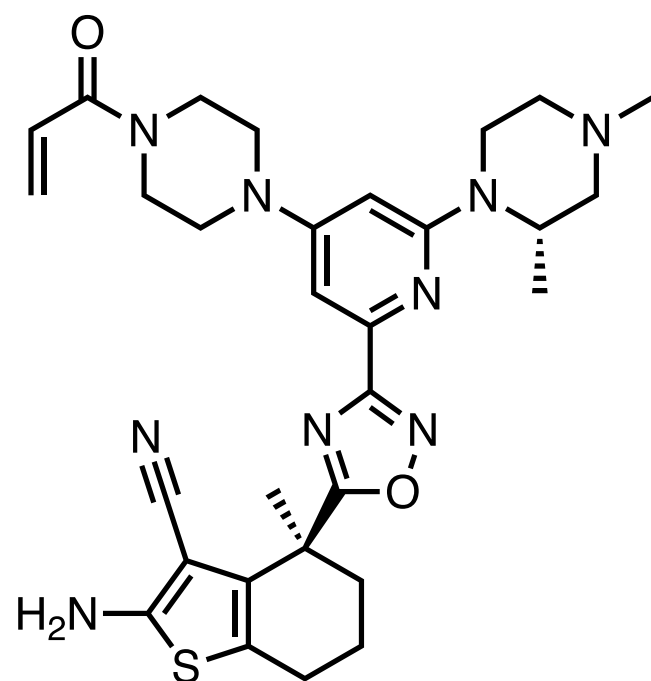


compound 12

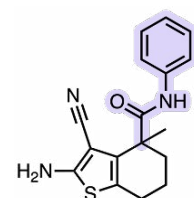
KRAS<sup>G12V,S39C</sup>-BIT  $K_D = <10 \mu\text{M}$

# BI-0474

KRAS<sup>G12C</sup>

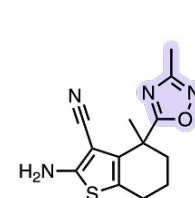


**Lead Optimization.** Optimization of “compound 12” began by growing the fragment toward Cys12, again using NMR as a screening strategy for KRAS<sup>G12V</sup> binding. Initial attempts focused on replacing the dimethyl moiety at position 4 with an amide (e.g., “compound 17b”,  $K_D = 1,180 \mu\text{M}$ ), but a significant loss of affinity was observed. When moving to the more rigid oxadiazole (“compound 19”,  $K_D = 20 \mu\text{M}$ ), affinity returned, albeit slightly weaker than for “compound 12”,  $K_D = 15 \mu\text{M}$ . Potency was restored by extending the ligand further toward Cys12 (“compound 20b”,  $K_D = <10 \mu\text{M}$ ). This was explained by an evaluation of the X-ray structure of “compound 12” (PDB:8AFC) and “compound 20a” (PDB:8AFD) in complex with GDP·KRAS<sup>G12C</sup>. A salt bridge between Glu62 and His95 that was present with “compound 12” had been broken by the aniline of “compound 20a”, explaining the initial drop in affinity with the amide series. However, the addition of an oxadiazole introduced a new H-bond between N-3 and His95, leading to an increase in affinity. Having hit the HSQC assay limit (10  $\mu\text{M}$ ), the use of an AlphaScreen assay, measuring the disruption of the GDP·KRAS<sup>G12C</sup>::SOS1 interaction, was implemented. Furthermore, acrylamide warheads were introduced to help further drive potency, using mass spectrometry to determine the rate of Cys12 modification. The X-ray structure of 20a suggested a linker between the warhead and the central phenyl core to position the acrylamide (“compound 22”) properly. X-ray analysis also suggested that a subpocket, formed by His95, Glu62, and Asp92, was available to further increase affinity. BI-0474 takes advantage of this subpocket by modifying the central phenyl ring to a pyridine (interaction with His95) and the introduction of a (3S)-1,3-dimethylpiperazine substituent.



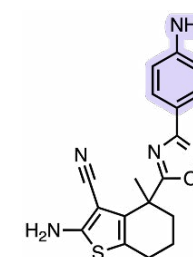
compound 17b

KRAS<sup>G12V</sup>  $K_D = 1,180 \mu\text{M}$



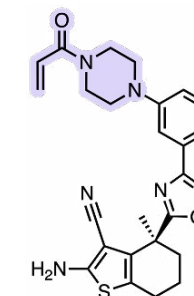
compound 19

KRAS<sup>G12V</sup>  $K_D = 20 \mu\text{M}$



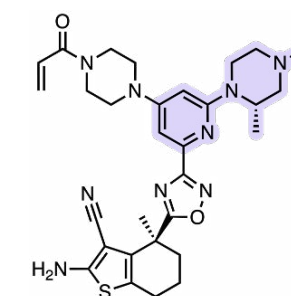
compound 20a

KRAS<sup>G12V</sup>  $K_D = <10 \mu\text{M}$



compound 22

KRAS<sup>G12C</sup>::SOS1  $IC_{50} = <3.3 \mu\text{M}$



BI-0474

KRAS<sup>G12C</sup>::SOS1  $IC_{50} = <3.3 \mu\text{M}$

**Binding Mode.** The crystal structure of BI-0474 in complex with GDP·KRAS<sup>G12C</sup> (PDB:8AFB) in the switch II pocket shows that this compound makes several interactions. In addition to the covalent bond with Cys12 residue, the crystalline structure revealed several direct hydrogen bonds and well water-mediated hydrogen bonds involving the nitrogen atoms of BI-0474 with Tyr64, Arg68, Glu62, His95, Asp92, and Asp69 residues.

**Preclinical Pharmacology.** In vivo experiments in NRMI nude mice coupled with an in silico PK model prediction suggested a target occupancy of >60% for the compound. In animals dosed with 40 mg/kg ip QD for three days, a 5-fold reduction in KRAS<sup>G12C</sup> levels was observed 2 h post-last dose, while a 9-fold reduction was seen 6 h post-last dose; a similar trend was observed with ERK levels, while treatment-induced apoptosis was also seen 6 h post-last dose. In an NCI-H358 NSCLC xenograft model, ip dosing of the drug at 40 mg/kg once or twice weekly resulted in a tumor growth inhibition of 68% or 98% on day 19 post-treatment, respectively. Some body weight loss ( $\leq 10\%$ ) in animals dosed with the compound vs. vehicle was observed, although this was less pronounced in animals receiving a lower dose.

**Clinical Development.** BI-0474 is a preclinical compound. However, an advanced oral compound from the series (BI 1823911) is currently being evaluated either alone or combined with other agents in a Ph. I study (NCT04973163) involving patients with advanced or metastatic cancer (including lung, colorectal, pancreatic, and bile duct cancers).

**Patent.** BI-0474 and its analogs were described in the patent WO2021245051A1. The US patent US20210380574A1 was filed by Boehringer Ingelheim and Vanderbilt University in June 2021 and is still pending.

IP KRAS<sup>G12C</sup>i related to oral candidate BI 1823911

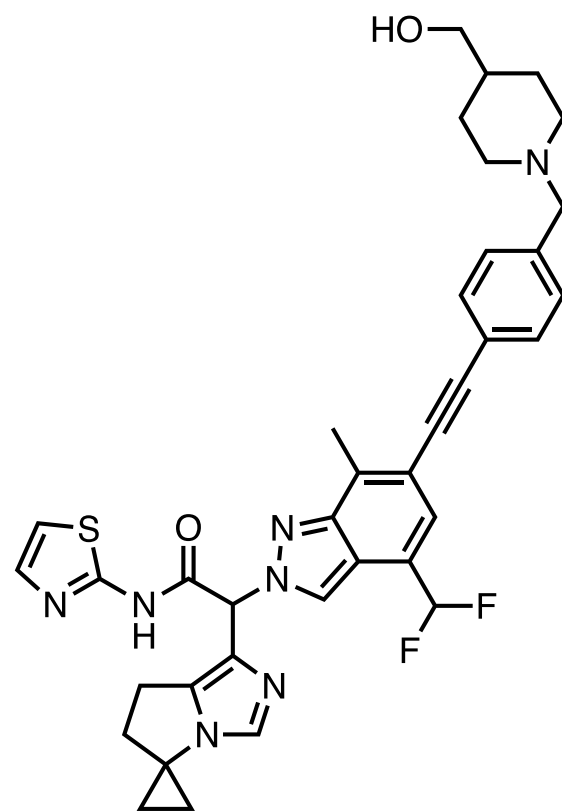
TGI in NCI-H358 cancer xenograft mouse model  
from 13k compd. HSQC-based screen and SBDD  
*J. Med. Chem.*

Boehringer Ingelheim, Vienna, AT

paper DOI: <https://doi.org/10.1021/acs.jmedchem.2c01120>

# compound 57

**EGFR<sup>L858R</sup>**



oral EGFR<sup>L858R</sup> inhibitor

efficacy in EGFR mutant mouse models

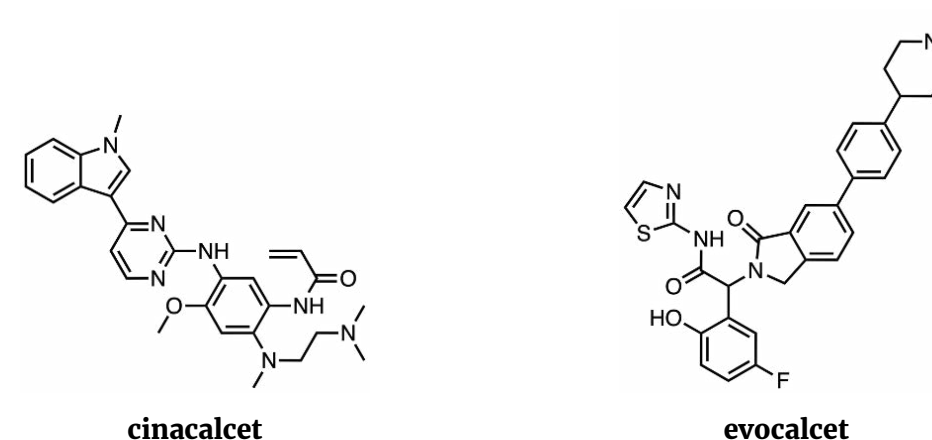
SBDD opt. from previously disclosed EGFRai

*J. Med. Chem.*

F. Hoffmann–La Roche, Basel, CH

paper DOI: <https://doi.org/10.1021/acs.jmedchem.2c00893>

**Context.** “[Compound 57](#)” (Roche) is an oral allosteric EGFR<sup>L858R</sup> inhibitor being developed for NSCLC. Drug resistance and associated disease relapse continue to remain unmet needs for patients with NSCLC tumors harboring EGFR mutations, despite the availability of [three generations of TKIs](#) for EGFR+ NSCLC. Although the widely used third-generation agent [osimertinib](#) has been highly effective against the commonly occurring T790M mutation, the exon 19 deletion (ex19del), and the L858R sensitizing mutations, the drug has been largely inactive against the [C797S-acquired mutation](#). Consequently, fourth-generation TKIs interact with an allosteric site generated by the L858R mutation, unlike current generation ATP-competitive agents. The newest class of inhibitors are actively being explored for treatment of L858R/C797S-, L858R/T790M-, or L858R/T790M/C797S-mutant EGFR. We previously highlighted [JBJ-09-063](#) (Dana-Farber), an allosteric EGFR TKI that was effective both as a single therapy and in combination with osimertinib against the L858R/T790M double and L858R/T790M/C797S triple mutants. However, JBJ-09-063 activity is reliant on the presence of the T790M “gatekeeper” mutation. Therefore, efforts to uncover an allosteric inhibitor with comparable efficacy with the L858R/T790M/C797S and L858R/C797S mutants independent of the T790M mutation have been underway.



cinacalcet

evocalcet

**Target.** [EGFR mutations in NSCLC](#) that mediate resistance to currently approved TKIs have been extensively studied. Notable resistance mutations include the [sensitizing ex19del and the L858R mutations](#), the [T790M mutation](#) that is present in up to 70% of cases and mediates resistance to first- and second-generation TKIs, and the [C797S mutation](#) that mediates resistance to the third-generation agent osimertinib. Acquisition of the C797S mutation results in [the formation of further mutations](#) L858R/C797S and ex19del/C797S or triple mutations such as L858R/T790M/C797S and ex19del/T790M/C797S. Roche scientists desired a compound with balanced activity across the different mutants which demonstrated activity even in mutants not harboring T790M mutations (i.e., L858R/C797S).

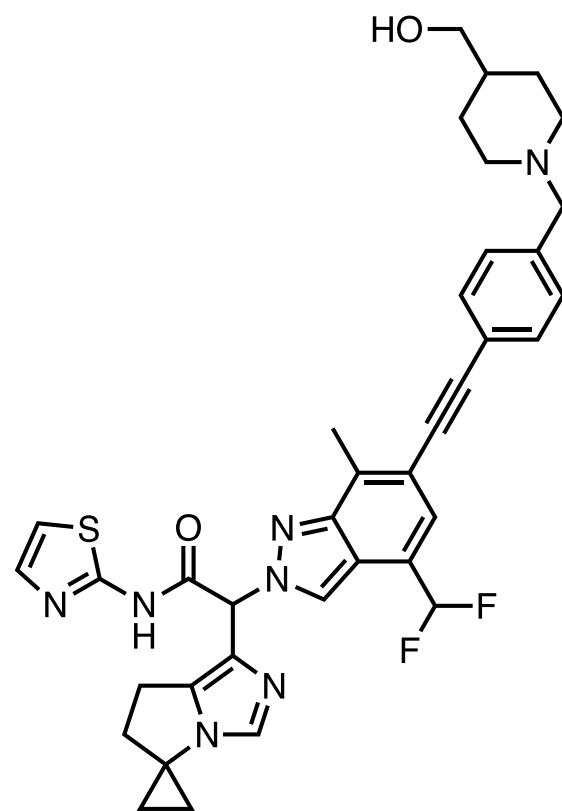
**Mechanism of Action.** Allosteric inhibitor (EGFRai) against the EGFR<sup>L858R</sup> or EGFR<sup>L858R/T790M</sup> mutations.

Allows for combination with orthosteric inhibitors as a strategy to overcome drug resistance in the second-line.

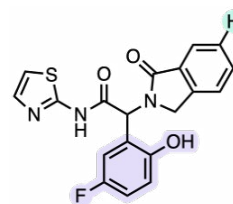
**Hit-Finding and Hit-to-Lead Strategy.** “Compound 57” was discovered in a fourth-generation campaign to address resistance to third-generation EGFR TKIs, including [EAI045](#) and [JBJ-04-125-02](#). EAI045, a single-digit nanomolar inhibitor of the L858R/T790M mutant with 1000-fold selectivity over the WT EGFR (1 mM of ATP), was optimized from the original hit, EAI001, discovered in a [2.5 million compound library](#) screen. Despite the high potency and selectivity of EAI045, it failed to achieve single-agent antitumor activity in vivo, due to EGFR mutant asymmetric dimerization that effectively blocks the allosteric binding site. The addition of a phenylpiperazine on the 6-position of the isoindoline resulted in a more potent [JBJ-04-125-02](#) with subnanomolar activity against EGFR<sup>L858R/T790M</sup>, but both third-generation inhibitors are less active against gatekeeper mutation T790M by at least an order of magnitude.

# compound 57

EGFR<sup>L858R</sup>

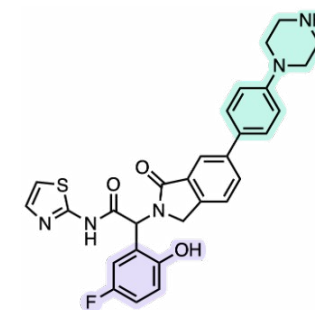


**Lead Optimization.** Lead optimization efforts focused on replacing the metabolically labile phenol with an imidazopyrrolidine and fine tuning of the substituent at the 6-position of the isoindoline to increase potency. The phenylacetylene replacement of the phenyl ring at the 6-position, and addition of both the methylene piperidine and methylene hydroxyl groups strongly increased potency in the EGFR<sup>L858R/C797S</sup> viability assay. The addition of the cyclopropyl group on the imidazopyrrolidine also increased potency in the viability assay. The isoindolinone core was replaced with a bioisosteric indazole and the CHF<sub>2</sub> group at the 4-position was an optimal lipophilic moiety that also increased potency. All modifications resulted in “compound 57” with a balanced profile for the double and triple mutants, but also a 1000X higher potency in the EGFR<sup>L858R/C797S</sup> viability assay.



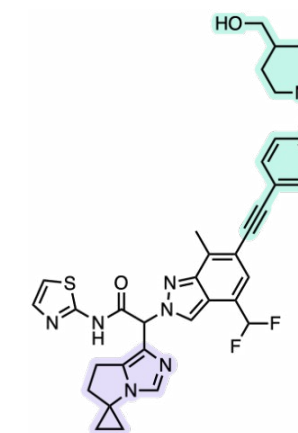
EAI045

WT EGFR IC<sub>50</sub> = 4300 μM  
EGFR<sup>L858R/T790M</sup> IC<sub>50</sub> = 3 nM



JBJ-04-125-02

EGFR<sup>L858R/T790M</sup> IC<sub>50</sub> = 0.26 nM  
pEGFR<sup>L858R/T790M/C797S</sup> IC<sub>50</sub> = 6 nM  
pEGFR<sup>L858R/C797S</sup> IC<sub>50</sub> = 460 nM



compound 57

pEGFR<sup>L858R/T790M/C797S</sup> IC<sub>50</sub> = 2 nM  
pEGFR<sup>L858R/C797S</sup> IC<sub>50</sub> = 20 nM

**Binding Mode.** The X-ray structure of “compound 57” complexed with the EGFR<sup>L858R/V948R</sup> mutant reveals how it achieves higher potency over other analogs via the positioning of difluoromethyl and cyclopentylimidazole moieties in the allosteric pocket (PDB:8A2D). The -CHF<sub>2</sub> group is positioned in a channel between Glu762 and Leu788, creating six short non-bonding interactions and a hydrogen bond with the carbonyl oxygen of Ile759. The cyclopentylimidazole makes a T-stacking interaction with a phenylalanine as well as one hydrogen bond with Arg858.

**Preclinical Pharmacology.** A Ba/F3 EGFR<sup>L858R/C797S</sup> allograft model was used for the in vivo efficacy and safety studies. Following oral BID dosing at 10 mg/kg, tumor growth inhibition of 84% was seen after 6 days of treatment and by day 20, 70% of animals had no measurable tumor. A 30 mg/kg BID dose was associated with poor tumor regression (26%). Combination therapy was explored with osimertinib in NCI-H1975 xenograft mice. The animals were dosed with “compound 57” (10 mg/kg BID), osimertinib (20 mg/kg QD), or osimertinib + “compound 57”. Single agent “compound 57” was associated with a tumor regression of 69% vs. 99% in single agent osimertinib. However, tumor regrowth was observed for both monotherapies 14 days after cessation of treatment. In animals dosed with the combination treatment, complete tumor regression was observed and 67% of the animals remained tumor-free following termination of the study. No significant body weight changes or safety concerns were reported.

**Clinical Development.** Preclinical compound.

**Patent.** “Compound 57” was disclosed in the patent [WO2022117477A1](#). Two additional patents describing several related indazole-based EGFR inhibitors were also disclosed ([WO2022117487A1](#), [WO2018115218A1](#)).

oral EGFR<sup>L858R</sup> inhibitor

efficacy in EGFR mutant mouse models

SBDD opt. from previously disclosed EGFR<sup>Rai</sup>

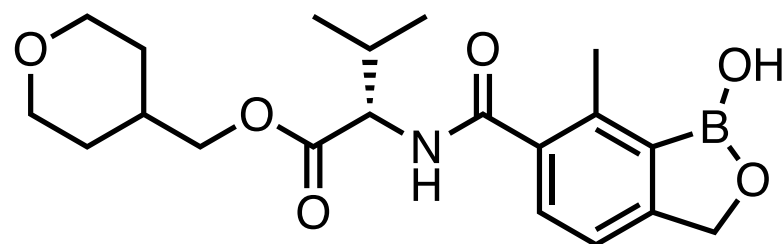
*J. Med. Chem.*

F. Hoffmann-La Roche, Basel, CH

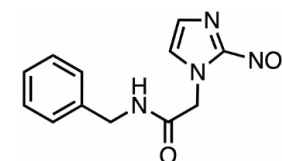
paper DOI: <https://doi.org/10.1021/acs.jmedchem.2c00893>

# AN15368

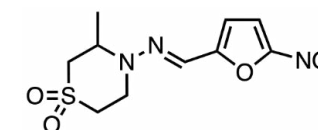
## CPSF3



**Context.** [AN15368](#) (Anacor Pharmaceuticals) is an oral cleavage and polyadenylation specificity factor (CPSF3) inhibitor being developed for Chagas disease, also known as American trypanosomiasis. [Chagas disease](#) is caused by *Trypanosoma cruzi* and is estimated to affect 6–7 million people worldwide, primarily those living in Latin America. The significant unmet need for additional Chagas disease treatments is underscored by the fact that the two currently FDA-approved therapies for the disease, Exeltis' first approved [benznidazole](#) and Bayer's [nifurtimox](#) (Lampit), are only indicated for pediatric patients due to [less conclusive efficacy data](#) as well as [safety/tolerability concerns](#) for adults. The highly potent and promising preclinical candidate AN15368 (in vitro  $IC_{50}$  = 5nM) was developed based on a [previously discovered](#) new class of boron-containing compounds (benzoxaboroles). A prodrug with an easy-to-hydrolyze ester group, AN15368 is cleaved by parasitic carboxypeptidases to yield the active drug as a free carboxylic acid (AN14667). It was demonstrated to inhibit the messenger RNA processing pathway in *T. cruzi*. during target identification studies and has already shown highly promising efficacy and safety in a clinical study in rhesus macaques. There has not been a novel drug approved for the prevention/treatment of Chagas disease [in over 50 years](#).



benznidazole

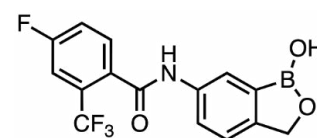


nifurtimox

**Target.** An optimized [genome-scale gain-of-function library](#) developed in trypanosomes was screened against promising benzoxaborole candidates, leading to the identification of CPSF3, an endonuclease that plays a key role in *T. cruzi* mRNA processing. Overexpression of the endonuclease in the parasite led to a 3–5-fold increase in resistance to AN15368 and cross-resistance to other benzoxaboroles, a result also observed in [additional studies](#). Further support for CPSF3 as the target of interest was demonstrated in a study that showed that the parasitic cells were resistant to AN15368 if an [Asn232 mutation was introduced in CPSF3](#), which disrupts the binding of benzoxaboroles in the parasite.

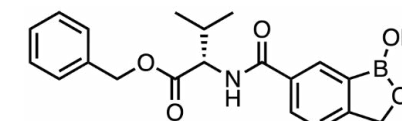
**Mechanism of Action.** Following activation by a *T. cruzi* serine carboxypeptidase, the product of AN15368 cleavage inhibits CPSF3-mediated mRNA maturation in intracellular amastigotes.

**Hit-Finding Strategy.** An early lead compound ([AN4169](#)) provided a functional cure of mice infected with a Brazilian strain of *T. cruzi*, however rodent tolerability studies suggested that there would be an insufficient therapeutic margin, so further progression was halted. In a follow up [study](#), several analogues of AN4169 were identified, with in vitro submicromolar activity against *T. cruzi* and good metabolic stability in an in vitro mouse S9 liver fraction assay. The most promising of these were AN10443 and AN11736, with AN11736 providing a [functional cure](#) in cattle infected with *T. congolense* or *T. vivax*, for a duration of 100 days. Their activity against *T. cruzi* was much lower.



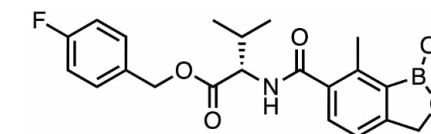
AN4169

*T. cruzi*  $IC_{50}$  = 350 nM



AN10443

*T. cruzi*  $IC_{50}$  = 670 nM



AN10443

*T. cruzi*  $IC_{50}$  = 0.9 nM

oral CPSF3 inhibitor for Chagas

uniformly curative in naturally infected rhesus macaques

from benzoxaborole library screen and opt.

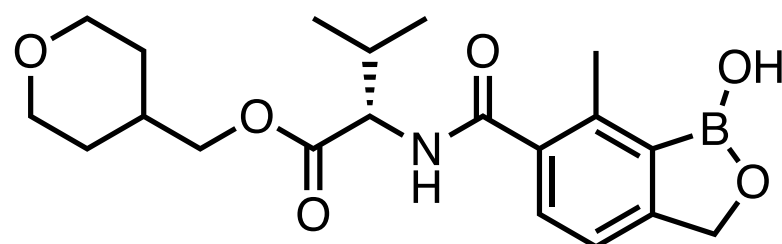
*Nat. Microbiol.*

Anacor Pharmaceuticals, Palo Alto, CA

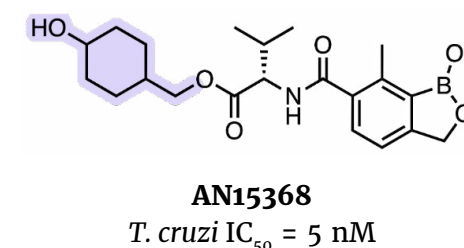
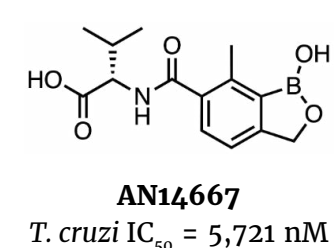
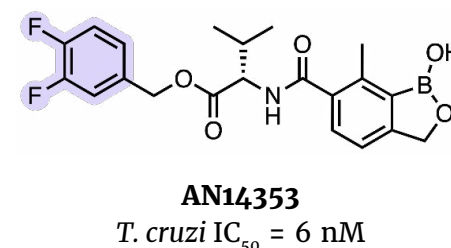
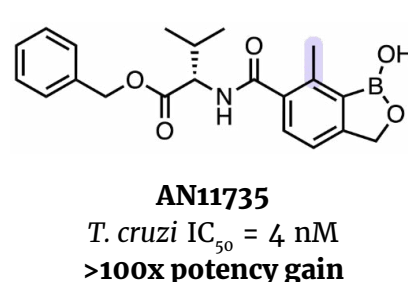
paper DOI: <https://doi.org/10.1038/s41564-022-01211-y>

# AN15368

## CPSF3



**Lead Optimization.** Optimization began by installing a methyl group at C(7) of the benzoxaborole ring of AN10443 ( $IC_{50} = 670$  nM); this dramatically increased in vitro activity against *T. cruzi* (AN11735,  $IC_{50} = 4$  nM). SAR studies on the benzyl ester showed little impact on potency, however, physicochemical properties and metabolic stability was quite variable, with metabolic stability tracking roughly with lipophilicity. This variability suggested further investigation of the ester region was warranted. In general, esters containing basic amines were less active than neutral compounds and small aliphatic compounds were generally quite potent ( $IC_{50}$  values  $<50$  nM). In vivo activity, following IV or oral dosing, was encouraging, with AN14353 ( $IC_{50} = 6$  nM) emerging as a prime candidate, based on its activity at lower doses. AN14353 showed rapid trypanocidal activity and high in vitro potency for a range of *T. cruzi* isolates, and consistently resolved established infections at a dose of 25 mg/kg in both wild-type and immunodeficient mice using a standard 40 d protocol. However, evaluation of the dose proportionality of exposure with AN14353 and generation of the active metabolite (AN14667) suggested solubility-limited absorption was occurring. Further optimization of aqueous solubility ultimately led to AN15368.



**Binding Mode.** X-ray crystal structure has not been disclosed.

**Preclinical Pharmacology.** C57BL/6J mice infected with *T. cruzi* and treated with the compound were subjected to a post-treatment terminal immunosuppression period to reveal residual infection. Following a 40-day treatment at 10 mg/kg, no parasite recovery or parasite DNA detection in skeletal muscle was seen. A similar activity was observed in an even more stringent treatment period of 20 days. In PK studies, the compound exhibited desirable dose-proportional exposure, and no hematotoxicity was observed below a 120 mg/kg dose, with insignificant effects at a 150 mg/kg dose. Furthermore, AN15368 was evaluated in a [non-human primate study](#) with 19 rhesus macaques positive for *T. cruzi*. Animals were treated with a 30 mg/kg dose for a 60 d period to mimic the treatment period used for humans, and the primary endpoint of the study was detection of parasite DNA in both blood and culture of blood parasites. Animals treated with AN15368 were uniformly cured, while 2 out of the 3 untreated animals were positive for the parasite. The study also found that AN15368 had an acceptable safety profile in animals.

**Clinical Development.** Preclinical compound.

**Patent.** AN15368 and related analogs were described in patent [WO2017195069A1](#). The US patent [US10562921B2](#) was granted to Anacor Pharmaceuticals in February 2020 and is valid until May 2037.

oral CPSF3 inhibitor for Chagas

uniformly curative in naturally infected rhesus macaques

from benzoxaborole library screen and opt.

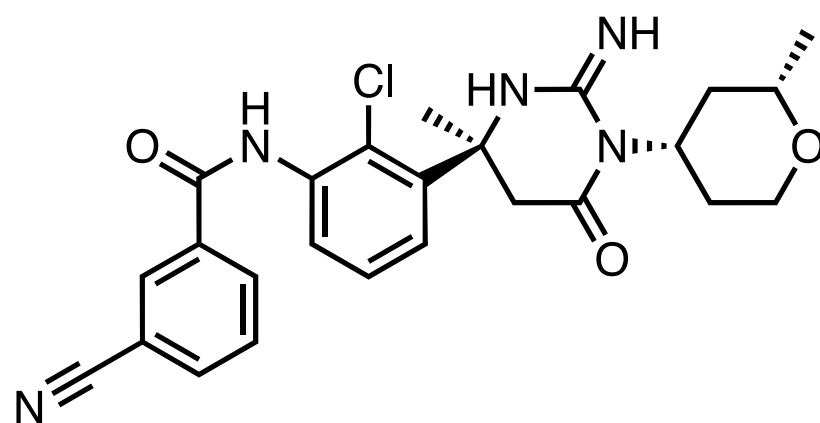
*Nat. Microbiol.*

Anacor Pharmaceuticals, Palo Alto, CA

paper DOI: <https://doi.org/10.1038/s41564-022-01211-y>

# UCB7362

## plasmepsin X

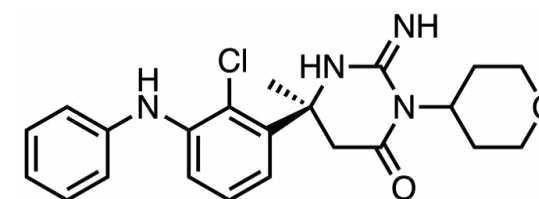


**Context.** [UCB7362](#) (UCB Biopharma) is an oral plasmepsin X (PMX) inhibitor being developed as an antimalarial agent. Malaria is a protozoan disease caused by *Plasmodium sp.* and remains a significant public health concern in many parts of the world, with [627,000 reported global deaths in 2020](#) despite the significant strides in the antimalarial drug space. [Artemisin-based combination therapies \(ACTs\)](#) are the standard in care for the disease, but increasing resistance to the therapy poses a significant challenge to treating and eradicating malaria. UCB7362 is a member of a novel class of compounds that target PMX, an aspartyl protease that plays a key role in *P. falciparum* egress. Structure-based optimization of a cyclic guanidine core, a privileged scaffold for aspartyl proteases, led to the discovery of UCB7362, which demonstrates in vivo efficacy and a half-life of 14 h. PK/PD modeling for the compound predicts a 50 mg daily dose for 7 consecutive days to cure, which may cause patient compliance issues where the current standard of treatment is a 3-dose regimen. Another potential liability is the poor selectivity UCB7362 has with [Cathepsin D \(Cat D\)](#) due to the shared [sequence homology](#) between plasmepsins and human aspartic proteases. Nonetheless, preclinical safety assessments in murine models did not reveal any ocultotoxic effects expected from off-target binding to Cat D, and the compound was well-tolerated overall.

**Target.** [Plasmepsin X](#) is one of 10 aspartic proteases produced by *P. falciparum* cells and plays a [known role in the parasite egress and invasion](#). PMX is expressed in the plasmodium blood-stage schizont and merozoite stage, as well as the gametocyte and liver stage of infection.

**Mechanism of Action.** Studies have shown the [importance of PMX and PMIX](#) in parasite egress and invasion. Specific PMX inhibition by UCB7362 results in inhibition of parasite growth, with the final maturation/egress of merozoites and reinfection of naïve human erythrocytes being the most drug-sensitive parasitic stages.

**Hit-Finding Strategy.** Cyclic acyl guanidines are privileged structures [known](#) to bind aspartyl proteases, with the guanidine core binding to the catalytic aspartic dyad in the substrate-binding site of the enzyme. A focused library was designed around this core and screened in a [FRET-labeled subtilisin-like serine protease 1 \(Pf SUB1\) peptide cleavage assay](#). The screen identified “compound 1” as a hit, with an  $IC_{50} = 15$  nM and both solubility (pH 5.8, 1057  $\mu$ M) and LogD (2.2) suitable for further optimization.



**compound 1**

$IC_{50} = 15$  nM

pH 5.8 solubility = 1057  $\mu$ M

LogD = 2.2

oral PMX inhibitor for malaria

50 mg QD/7 days estimated to be curative

from guanidine-based focused lib. screen. and SBDD

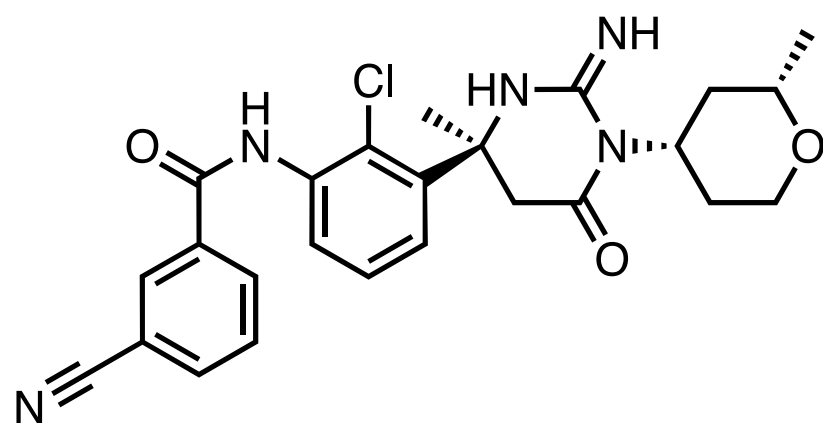
*J. Med. Chem.*

UCB Biopharma, Braine-l'Alleud, BE

paper DOI: <https://doi.org/10.1021/acs.jmedchem.2c01336>

# UCB7362

## plasmepsin X



oral PMX inhibitor for malaria

50 mg QD/7 days estimated to be curative

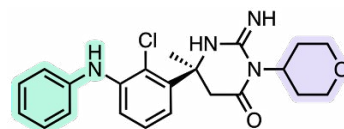
from guanidine-based focused lib. screen. and SBDD

*J. Med. Chem.*

UCB Biopharma, Braine-l'Alleud, BE

paper DOI: <https://doi.org/10.1021/acs.jmedchem.2c01336>

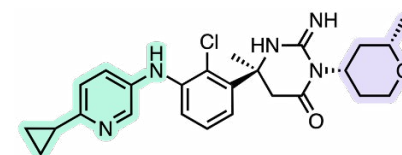
**Lead Optimization** Initial optimization of “compound 1” focused on reducing metabolic clearance by exchanging the labile benzene ring with a cyclopropyl pyridine and increasing potency with the specific *S,S*-tetrahydropyran stereochemistry to afford “compound 3” (PMX IC<sub>50</sub> = 7 nM). The observed human aspartyl protease promiscuity, including Cat D and renin, was a key issue with the privileged cyclic acyl guanidine scaffold. Efforts were placed on improving both the off-target safety profile (using a “[SafetyScreen 44](#)” panel) and the selectivity of “compound 3,” with IC<sub>50</sub> values of 64 and 180 nM for Cat D and renin, respectively. Remarkably, replacing the biarylamine with an amide greatly improved the selectivity against Cat D and renin (3,889 nM and >10,000 nM, respectively), and adding a cyano group on the benzene ring retained potency while further reducing off-target binding to 7%, to afford UCB7362.



**compound 1**

PMX IC<sub>50</sub> = 15 nM

CL<sub>int</sub> hep (hu) = 28 μL / min 10<sup>6</sup> cells

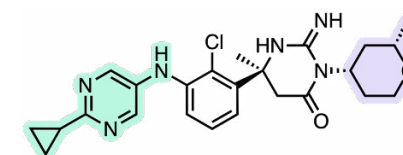


**compound 3**

PMX IC<sub>50</sub> = 7 nM

CL<sub>int</sub> hep (hu) = 6 μL / min 10<sup>6</sup> cells

off-target screen hit rate = 20%

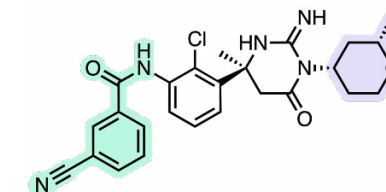


**compound 4**

PMX IC<sub>50</sub> = 9 nM

CL<sub>int</sub> hep (hu) = 4 μL / min 10<sup>6</sup> cells

off-target screen hit rate = 14%



**UCB7362**

PMX IC<sub>50</sub> = 7 nM

CL<sub>int</sub> hep (hu) = 4 μL / min 10<sup>6</sup> cells

off-target screen hit rate = 7%

**Binding Mode.** The binding mode of UCB7362 has not been disclosed. However, an X-ray crystal structure of closely related analog, “compound 4” (PDB:8DSR), revealed some interesting interactions. “Compound 4” binds with PMX at an orthosteric site with hydrogen bonding between the guanidine moiety and the catalytic aspartic acid diad (Asp457 and Asp266).

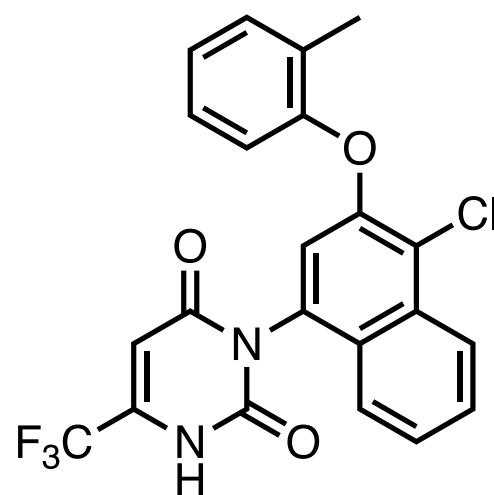
**Preclinical Pharmacology.** A [validated \*P. falciparum\* humanized murine model](#) was used for in vivo efficacy experiments. The compound was dosed BID at 10, 25, and 60 mg/kg for 4 days, with positive control animals receiving 10 mg/kg of chloroquine. By day 4, in the animals dosed at 60 mg/kg, parasitemia levels were found below the quantitation limit (QL), and levels stayed below the QL through day ~18 before increasing to baseline levels by day ~27. In animals dosed with chloroquine, clearance of parasitemia to below the QL was seen on day 5, but levels increased again around day 7 and reached baseline levels by day ~13. The recrudescence period (duration of response) was investigated through PK/PD experiments, which suggested that an important driver of efficacy was the total time above a threshold concentration in blood. Animals that received a compound exposure <96 h were found to demonstrate recrudescence. This suggests that a minimum duration of exposure of the drug must be met for curative effects to be achieved. Safety assessments did not reveal any cytotoxicities at concentrations up to 100 μM. Despite the finding that UCB7362 has off-target effects on human Cat D, the compound did not demonstrate any ocular toxicities in animals.

**Clinical Development.** Preclinical compound.

**Patent.** UCB7362 and related antimalarial compounds were disclosed in the patent [WO2019192992A1](#). The US patent [US20210094941A1](#) was filed by UCB Biopharma in April 2019 and is still pending.

# BAY-069

## BCAT1/2



**Context.** [BAY-069](#) (Bayer) is a branched-chain amino acid transaminase (BCAT) 1/2 inhibitor. Involved in the synthesis and breakdown of branched-chain amino acids, [BCAT1 and BCAT2](#) have also been implicated in several diseases, including various cancer types, with the ligandability evidenced by the [many reported inhibitors](#). Tool compound BAY-069, a (trifluoromethyl)pyrimidinedione identified in an HTS campaign, is a BCAT1-focused dual BCAT1/2 inhibitor with  $IC_{50}$  values of 31 nM for BCAT1 and 153 nM for BCAT2. Donated by BI as a chemical probe along with an inactive control, it may be helpful to further understand BCAT biology and safety in different settings. The molecule is an interesting example of an oral molecule with an  $N2$ -substituted pyrimidinedione.

**Target.** [BCATs](#) mediate the catabolism of the branched-chain amino acids valine, leucine, and isoleucine to branched-chain keto acids. [BCAT1 and BCAT2](#) are the two known family members, with BCAT1 being expressed in the cytoplasm of some tissues and BCAT2 being ubiquitously expressed in mitochondrial tissues. BCAT has been [implicated](#) in the pathogenesis of tumors, Alzheimer's disease, myeloid leukemia, and other diseases. Specifically, cytoplasmic BCAT1 has been found to be [overexpressed in several cancers](#) and may even be [involved in chemoresistance](#), while mitochondrial BCAT2 has also been found to [regulate ferroptotic cell death](#) in tumor cells. In cancer, BCAT promotes cellular proliferation and invasion by [activating](#) the phosphatidylinositol 3-kinase (PI3K)/protein kinase B, (PKB; Akt)/mammalian target of rapamycin (mTOR) pathway and Wnt/ $\beta$ -catenin signaling. The suitability of BCAT1/2 as drug targets has been demonstrated by several known [inhibitors](#).

**Hit-Finding Strategy.** Two BCAT1/2 inhibitors ("compound 1", BCAT1  $IC_{50}$  = 554 nM, BCAT2  $IC_{50}$  = 13,300 nM, and "compound 2", BCAT 1  $IC_{50}$  = 3,300 nM and BCAT2  $IC_{50}$  = 20,000 nM) were identified from a high-throughput screen of 788,762 compounds from Bayer's in-house library. The assay measured BCAA  $\alpha$ -ketoisocaproate reduction to leucine by using leucine dehydrogenase (LeuDH) to catalyze the NADH-dependent transformation. This screen revealed 2,183 primary hits, of which 838 were specific, and 399 had an  $IC_{50}$  below 20  $\mu$ M. "Compound 1" had a modest Caco-2 intestinal permeability (30.0 nm/s) and an efflux ratio of 6.2, and was chosen for further optimization.

oral BCAT1/2 inhibitor

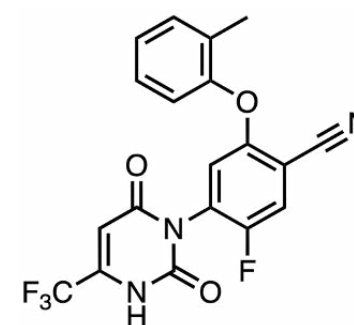
favorable PK profile in rats

from 788762 compd. HTS and SBDD

*J. Med. Chem.*

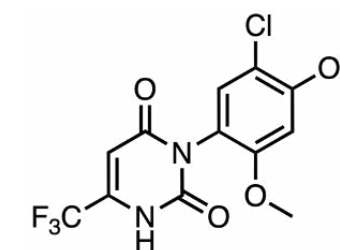
Bayer Pharma AG, Berlin, DE

paper DOI: <https://doi.org/10.1021/acs.jmedchem.2c00441>



**compound 1**

BCAT1  $IC_{50}$  = 554 nM  
BCAT2  $IC_{50}$  = 13,300 nM

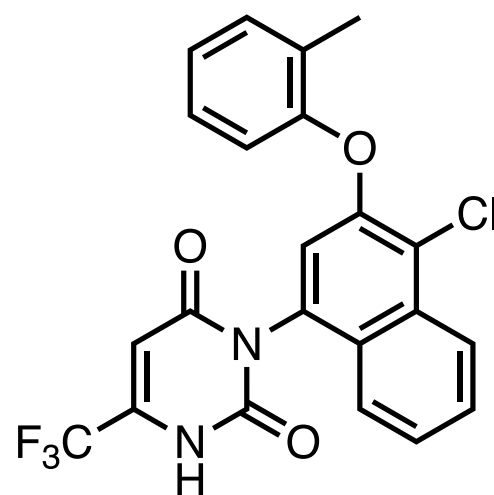


**compound 2**

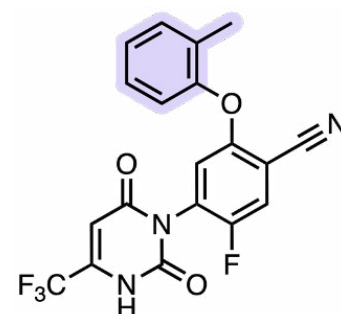
BCAT1  $IC_{50}$  = 3,300 nM  
BCAT2  $IC_{50}$  = 20,000 nM

# BAY-069

## BCAT1/2

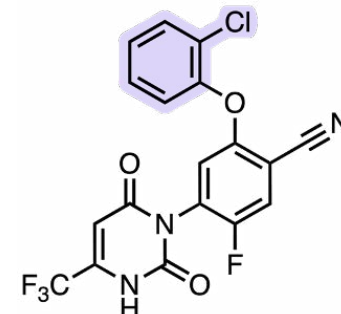


**Lead Optimization.** X-ray analysis of “compound 1” in complex with BCAT1 indicated binding occurred within the active site, directly in front of the PLP cofactor, where its toluyl moiety inserts into the hydrophobic section of the binding pocket and an H-bond is formed between one of the carbonyl oxygens and Val175. Initial SAR optimization of the toluyl region showed modest improvements in BCAT1 potency, while BCAT2 potency was improved by an order of magnitude (e.g., “compound 8”). Further analysis of the X-ray structure of “compound 1” suggested that larger substituents at the 5-position of the central benzene core might fill the corresponding part of the binding pocket (e.g., “compound 35”). Interestingly, “compound 35” exists as a racemic mixture of separable **atropisomers** (results shown for racemate). Although the  $IC_{50}$  values for “compound 35” were encouraging, permeability and efflux remained an issue. Ultimately, replacement of the nitrile with a chloride solved this problem, leading to BAY-069, which was isolated as a single atropisomer (no stereochemistry shown). BAY-069 demonstrates a good Caco-2 permeability of 252 nm/s, a good efflux ratio of 0.48, and good clearance of 122 L/h/kg.



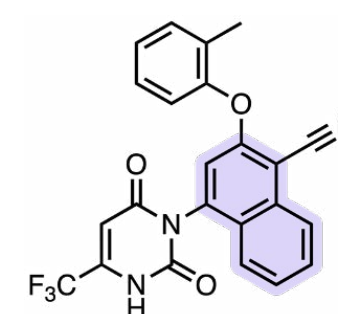
**compound 1**

BCAT1  $IC_{50}$  = 554 nM  
BCAT2  $IC_{50}$  = 13,300 nM  
Caco-2  $P_{app}$  A-B = 30 nm/s  
efflux ratio = 6.2



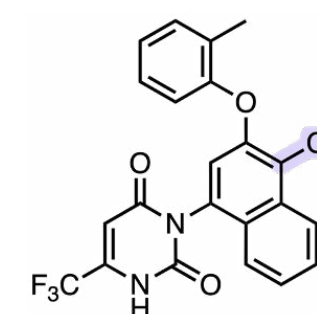
**compound 8**

BCAT1  $IC_{50}$  = 159 nM  
BCAT2  $IC_{50}$  = 1,680 nM



**compound 35**

BCAT1  $IC_{50}$  = 70 nM  
BCAT2  $IC_{50}$  = 270 nM  
Caco-2  $P_{app}$  A-B = 13 nm/s  
efflux ratio = 11.1



**BAY-069**

BCAT1  $IC_{50}$  = 31 nM  
BCAT2  $IC_{50}$  = 153 nM  
Caco-2  $P_{app}$  A-B = 252 nm/s  
efflux ratio = 0.48

**Binding Mode.** The X-ray structure of BAY-069 complexed with BCAT1 (**PDB:7NYA**) shows that the inhibitor binds within the active site pocket, in front of the PLP cofactor. The naphthalene moiety is positioned in a hydrophobic pocket between Tyr193 and Phe49 sidechains, and engages in a  $\pi$ - $\pi$  stacking interaction with the latter. Other relevant interactions include hydrogen-bonding of the pyrimidinedione core with the Val175, Tyr193, and Gln244 residues.

**Preclinical Pharmacology.** Rats dosed at 0.3 mg/kg IV or 0.6 mg/kg PO demonstrated favorable PK characterized by low clearance (0.64 L/h/kg; IV), moderate steady-state volume of distribution (0.25 L/kg; IV), a half-life of 1.6 h (IV), and high oral bioavailability (89%). In vivo efficacy and safety data have yet to be reported.

**Clinical Development.** Preclinical compound.

**Patent.** BAY-069 and related pyrimidinedione derivatives were described in the patent **WO2021063821A1**. A US patent has not been disclosed.

oral BCAT1/2 inhibitor

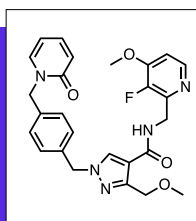
favorable PK profile in rats

from 788762 compd. HTS and SBDD

*J. Med. Chem.*

Bayer Pharma AG, Berlin, DE

paper DOI: <https://doi.org/10.1021/acs.jmedchem.2c00441>

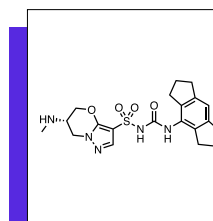
**sebetralstat | plasma kallikrein**

oral, on-demand plasma kallikrein inhibitor  
Ph. III candidate for on-demand treatment  
of HAE attacks

opt. from a known starting point

*J. Med. Chem.*

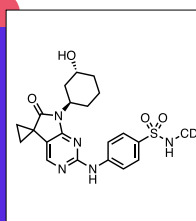
KalVista Pharmaceuticals Ltd., Salisbury, U.K.

**GDC-2394 | NLRP3**

oral NLRP3 inhibitor  
predicted human dose of 500 mg QD  
LLE opt. and tox. mitig. from prev. clin. cand.

*J. Med. Chem.*

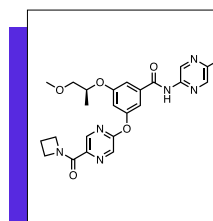
Genentech, South San Francisco, CA

**compound 5g | CDK2**

oral CDK2 Inhibitor  
oral/IV PK observed in rats  
in-house HTS and scaffold hopping

*ACS Med. Chem. Lett.*

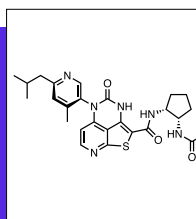
Incyte Research Institute, Wilmington, DE

**AZD1656 | glucokinase**

oral glucokinase activator  
Ph. II in renal transplant patients with DM2  
AZD1092 opt. to avoid Ames test liability

*Sci. Transl. Med.*

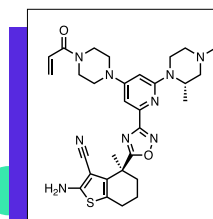
AstraZeneca, Gothenburg, SE

**JNJ-64264681 | BTK**

oral BTK inhibitor  
Ph. I candidate in NHL/CLL patients  
from Janssen cmp. collection screen and opt.

*J. Med. Chem.*

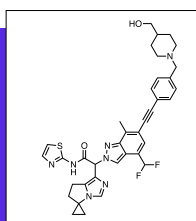
Janssen, San Diego, CA

**BI-0474 | KRAS<sup>G12C</sup>**

IP KRAS<sup>G12C</sup> related to oral candidate BI 1823911  
TGI in NCI-H358 cancer xenograft mouse model  
from 13k cmpd. HSQC-based screen and SBDD

*J. Med. Chem.*

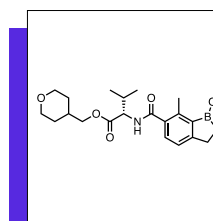
Boehringer Ingelheim, Vienna, AT

**compound 57 | EGFR<sup>L858R</sup>**

oral EGFR<sup>L858R</sup> inhibitor  
efficacy in EGFR mutant mouse models  
SBDD opt. from previously disclosed EGFRai

*J. Med. Chem.*

F. Hoffmann-La Roche, Basel, CH

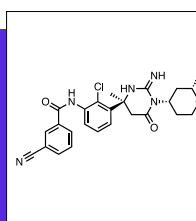
**AN15368 | CPSF3**

oral CPSF3 inhibitor for Chagas  
uniformly curative in naturally infected  
rhesus macaques

from benzoxaborole library screen and opt.

*Nat. Microbiol.*

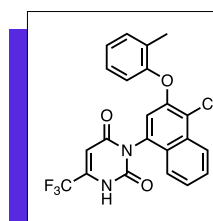
Anacor Pharmaceuticals, Palo Alto, CA

**UCB7362 | plasmepsin X**

oral PMX inhibitor for malaria  
50 mg QD/7 days estimated to be curative  
from guanidine-based focused lib. screen.  
and SBDD

*J. Med. Chem.*

UCB Biopharma, Braine-l'Alleud, BE

**BAY-069 | BCAT1/2**

oral BCAT1/2 inhibitor  
favorable PK profile in rats  
from 788762 cmpd. HTS and SBDD

*J. Med. Chem.*

Bayer Pharma AG, Berlin, DE

**discover together**

[drughunter.com](http://drughunter.com)  
[info@drughunter.com](mailto:info@drughunter.com)